Electric Power Systems Research
Peer-reviewed and accepted version

Simulation and Evaluation of Zonal Electricity Market Designs

Mahir Sarfati, Pär Holmberg

Published version:
https://doi.org/10.1016/j.epsr.2020.106372

Research Institute of Industrial Economics
P.O. Box 55665
SE-102 15 Stockholm, Sweden
info@ifn.se
www.ifn.se

Simulation and Evaluation of Zonal Electricity Market Designs

M. Sarfati[a,b], P. Holmberg[b,c,d]

[a]KTH Royal Institute of Technology, Sweden
[b]Research Institute of Industrial Economics (IFN), Sweden
[c]Energy Policy Research Group (EPRG), University of Cambridge, UK
[d]Program on Energy and Sustainable Development (PESD), Stanford University, CA, USA

Abstract

Zonal pricing with countertrading (a market-based redispatch) gives arbitrage opportunities to the power producers located in the export-constrained nodes. They can increase their profit by increasing the output in the day-ahead market and decrease it in the real-time market (the inc-dec game). For a six-node and a 24-node system, we numerically show that this leads to large inefficiencies in a standard zonal market. We also show how the inefficiencies can be significantly mitigated for these two examples by changing the design of the real-time market. We consider a two-stage game with oligopoly producers, wind-power shocks and real-time shocks. The game is formulated as a two-stage stochastic Equilibrium Problem with Equilibrium Constraints (EPEC), which we recast into a two-stage stochastic Mixed-Integer Linear Constraints (MILC).

Keywords: Two-stage game, Zonal pricing, Wholesale electricity market

1. Introduction

Over the last two decades, a number of countries have deregulated their electricity industry in order to create competitive electricity markets. These markets have different methodologies to handle transmission congestion. The US and some other countries use nodal pricing while Europe and Australia have favored zonal pricing. Nodal pricing explicitly considers the transmission constraints and all accepted bids are paid with the local price in the node where the participant is located. Zonal pricing is an approximation of the nodal pricing regime. It aggregates specific nodes in order to create zones with uniform prices. Compared to nodal pricing, the zonal approximation would normally lead to a less efficient day-ahead dispatch. On the other hand, it could be argued that zonal pricing simplifies clearing of the day-ahead market and that it facilitates hedging and intra-day trading, see Ahlqvist et al. (2018). Moreover, market participants, especially consumers, often favor zonal pricing.

We consider zonal markets where all stages are market based, as in UK. The first stage is the day-ahead market. In the economic dispatch related to the day-ahead market, each zone is assumed to be a copper plate and only transmission constraints between zones are considered. The second stage is the real-time market, where all transmission constraints are fully represented in the economic dispatch problem. The simplified representation of transmission constraints in the day-ahead market may cause overloading of some of the transmission lines.

Email addresses: `sarfati@kth.se` (M. Sarfati), `par.holmberg@ifn.se` (P. Holmberg)

This is relieved by counter-trading in the real-time market; the system operator accepts bids which reduce the production in the export constrained nodes and accepts bids which increase the production in the import constrained nodes.

Different representations of the transmission constraints in the two stages give different prices in the two stages. This gives producers an arbitrage opportunity. Harvey and Hogan (2000a) and Harvey and Hogan (2000b) show that a producer in an export constrained node can increase its profit by selling more in the day-ahead market and then buy back power at a lower price in the real-time market. This kind of bidding behavior is referred to as the *increase-decrease (inc-dec) game*. As explained by Alaywan et al. (2004) this game contributed to the electricity crisis in California and to that California and other markets in the US switched from zonal to nodal pricing. According to Neuhoff et al. (2011), there are also problems with the inc-dec game in the British electricity market. EU is currently pushing for market-based redispatches and wants to increase cross-border flows (the 70 % rule). System operators in Europe are worried that these changes will increase the inc-dec problem. As an example, Hirth et al. (2019) estimate that, due to the inc-dec game, the transacted volume in the German real-time market would increase by 3-7 times, if Germany would introduce a market-based redispatch. In this paper, we develop mathematical models to quantify inefficiencies and other problems related with zonal pricing. We also present a new real-time market design which can potentially mitigate these problems. At least it significantly reduces the inc-dec problems for the two networks that we simulate.

Several researchers have analyzed the zonally-priced electricity markets. Green (2007), Bjørndal and Jörnsten (2007) and Bjørndal et al. (2012) consider a one-stage game of a whole-sale market with zonal pricing. Ruderer and Zöttl (2012) consider a regulated (non-market based) redispatch without the inc-dec game, as in the German electricity market. Bjørndal et al. (2013) analyze market power in zonal electricity markets with a day-ahead stage and a re-dispatch stage. They assume that all producers are price-takers in the day-ahead stage and accordingly, they ignore arbitrage possibilities and the inc-dec game. Holmberg and Lazarczyk (2015) make an analytical comparison of nodal, zonal and discriminatory pricing and conclude that even if the optimal dispatch of the producers are the same in all pricing approaches, the inc-dec game results in extra profit for the producers located at the export-constrained nodes. Holmberg and Lazarczyk (2015) disregard imperfect competition and focus on imperfections caused by arbitrage opportunities. Dijk and Willems (2011) consider both imperfect competition and arbitrage opportunities but their analytical analysis is limited to two-node networks. They show that the extra profit for export constrained producers distorts the investment signals and this causes a long-run social welfare loss.

It is known that the inc-dec game can be mitigated by making the day-ahead market more similar to the real-time market. As in the US reforms, this can for example be done by introducing nodal pricing in the day-ahead market, so that all network constraints are considered already day-ahead. An observation made in this paper is that it should also be possible to reduce arbitrage opportunities by making the real-time market more similar to a zonal day-ahead market. Hence, we would like to investigate whether making the real-time market more similar to a zonal day-ahead market could improve efficiency for zonal markets. This is one of the contributions of this paper. We study this for two systems with multiple nodes and imperfect competition.

We assume that each producer chooses a bid price for its plant[1] and in our simulations we consider two different methods to set prices in the real-time market: (i) pay-as-bid pricing as in Britain and (ii) optimal zonal pricing. Optimal zonal pricing means that all constraints of the network are considered by the real-time market, but we add an extra constraint which requires that the clearing price must be the same for all nodes within a zone. Bjørndal and Jørnsten (2001) and Bjørndal et al. (2012) apply the optimal zonal pricing concept to the day-ahead market[2]. The extra constraint in the real-time market would, all else equal (including all bids), make the design less efficient. In our model, it will be particularly inefficient to introduce this constraint, because the system operator will sometimes need to spill wind to uphold the zonal constraint. On the other hand, the zonal constraint makes the real-time market more similar to a day-ahead zonal market. This reduces price differences between the day-ahead and real-time market, which mitigates the inc-dec game. Overall, the market efficiency improves substantially in our two examples, compared to our model of the British design. In one of our examples, optimal zonal pricing is roughly as efficient as nodal pricing, which we use as a benchmark.

We formulate the two-stage price game as a two-stage stochastic Equilibrium Problem with Equilibrium Constraints (EPEC). The two-stage stochastic EPEC is reformulated as a set of Mixed-Integer Linear Constraints (MILC)[3]. A feasible point which satisfies the developed MILC model is a Subgame Perfect Nash Equilibrium (SPNE) of the two-stage game. The algorithm is explained in more detail in a parallel paper, Sarfati et al. (2018a), that studies the inc-dec game for a zonal market of the Nordic type.

In this study, we consider net-demand uncertainties in the day-ahead market and we compare the welfare of electricity markets where the real-time market design is either pay-as-bid pricing or optimal zonal pricing. The set of permissible price bids is discrete in our model. This means that we have the set of equilibria under control. We can, in principle, solve for all SPNE, and we can verify that all best responses are global best responses. We propose two methodologies to manage multiple equilibria. The first methodology applies a iterative procedure and finds all SPNE of the game. This methodology is relevant for small-scale examples where the computation of the MILC model takes shorter time. The second methodology for tackling multiple SPNE, which we also use in Sarfati et al. (2018b), is to build a SPNE band. The SPNE band is divided into several subintervals and a representative SPNE is found in each subinterval. This methodology allows us to find a set of representative SPNE with controlled tolerance. The developed MILC model and the two methodologies to tackle multiple SPNE are demonstrated on a 6-node system and the IEEE 24-node example system for the alternative market designs that we consider.

In our model, the market/system operator makes sure that there is a feasible dispatch for any combination of bids. Thus similar to Willems (2002), we can avoid equilibrium ambigu-

[1]In this paper, we consider a price-bid or Bertrand game. However, in principle our approach could be changed to the Cournot game (quantity-bid game) or price-quantity-bid game as in Hesamzadeh and Biggar (2012) and Hesamzadeh and Biggar (2013).

[2]This is related to flow-based market coupling, see van den Bergh et al. (2016), which Central Western Europe (CWE) has introduced in the day-ahead electricity market. Sarfati et al. (2019) study the inc-dec game in markets with flow-based zonal pricing in the day-ahead market.

[3]In previous version of this paper, Hesamzadeh et al. (2018), we reformulate the two-stage stochastic EPEC model as a mixed-integer nonlinear program which requires a special algorithm to compute the global optimal solution.

ities and the Generalized Nash equilibrium concept. These are well-known issues in Cournot games where the move of one player directly sets its own output and therefore constrains the permissible moves of other players in capacity constrained transmission networks, as explained by Stoft (1999).

More broadly, our method is related to previous studies of EPEC problems. Zhang and Xu (2013) analyze numerical methods that can be used to solve for a two-stage stochastic EPEC. Zhang et al. (2010) use a Cournot model and Zhang and Kim (2010) a linear supply function equilibrium model to study the strategic behavior of producers that participate in a forward and day-ahead market without transmission constraints. Zhang and co-authors formulate their models as mixed-complimentarity problems, which are either solved using the PATH solver or reformulated as a NLP problem. Holmberg and Willems (2015) consider a related problem where producers sell a portfolio of option contracts in the first stage and then compete with supply functions in the spot market. They consider a problem with symmetric producers and are able to solve the problem analytically. One contribution by Holmberg and Willems (2015) to the EPEC literature is that it establishes conditions for which solutions to EPEC problems are SPNE for games with a continuous strategy space. Hu and Ralph (2007) analyze bilevel games for spot markets with nodal pricing. In an EPEC model, several agents make rational decisions in each stage. This is a generalization of a Mathematical Program with Equilibrium constraints (MPEC), see Moiseeva and Hesamzadeh (2018). An MPEC models a situation where only one agent makes a decision in the first stage and several agents make rational decisions in the second stage, as in a Stackelberg game.

The main contribution of this work is fourfold: (i) We put forward the conjecture that the inc-dec game can be mitigated by making the design of real-time markets more similar to a zonal day-ahead market. (ii) As a theoretical test of such a design, we propose that optimal zonal pricing can be used in the real-time market. It considers all constraints of the network and an extra constraint which requires that the clearing price in the real-time market must be the same for all nodes within a zone. (iii) We model a two-stage price-bid game to analyze zonal markets considering two different real-time pricing approaches: (a) pay-as-bid pricing as in Britain and (b) optimal zonal pricing. The two-stage price-bid game is formulated as a two-stage stochastic EPEC. Then it is reformulated as a two-stage stochastic MILC model. (iiii) We simulate two networks where optimal-zonal pricing in the real-time market significantly mitigates the inc-dec game.

This paper is organized as follows: The two-stage game and the market designs considered in this study are explained in section 2. Section 3 derives the mathematical model of the two-stage game. Section 4 presents two methodologies to tackle the multiple-SPNE issue. Sections 5 and 6 demonstrate the application of the mathematical model on a 6-node and the IEEE 24-node example systems. Section 7 concludes the paper.

2. Description of two-stage game

We consider a two-stage electricity market which employs zonal pricing. The first stage is the day-ahead market and the second one is the real-time market. We assume that both markets are physical and that oligopolistic producers participate in both markets.

The competition in a two-stage electricity market is modeled as a two-stage game under uncertainty. In the first stage, each producer chooses its day-ahead bid considering the presumed day-ahead decisions of its rivals and the Nash equilibrium in the real-time market. After producers submit their optimal day-ahead bids, the net-demand uncertainty (ω) is realized and revealed to all producers. In the second stage, each producer chooses its real-time bids (up-regulation and down-regulation bids) given the day-ahead dispatch results and the presumed real-time bids decisions of its rivals and submits it to the system operator. The system operator clears the real-time market after the net-demand shocks ($s|\omega$) have been realized.

In this study, we consider two different pricing approaches in the real-time market which are summarized in Table 1. Approach 1 assumes that all accepted bids in the real-time market are paid their bid price as in the real-time market in Britain. In Approach 2, the real-time market applies optimal zonal pricing. This means that all constraints of the network are considered by the real-time market, but we add an extra constraint which requires that the clearing price must be the same for all nodes within a zone. We assume that all accepted bids in the real-time market are paid with the marginal zonal price (MZP). One of our purposes with this pricing approach is that it should give similar prices as in the day-ahead market. This should reduce arbitrage opportunities and mitigate the inc-dec game.

Table 1: Zonal pricing in the real-time market, up-reg: Up-regulation, dn-reg: Down-regulation, no-reg.: no regulation, PAB: Pay-as-bid, MZP: Marginal zonal price

	Accepted bid			
System need	Approach 1		Approach 2	
	up-reg.	dn-reg.	up-reg.	dn-reg.
up-reg.	PAB	PAB	MZP	MZP
dn-reg.	PAB	PAB	MZP	MZP
no-reg.	PAB	PAB	MZP	MZP

2.1. Introductory Two-Node Example

We use a simple two-node example, see Fig. 1, to illustrate the inc-dec game and the considered market designs. Assume that there is one producer with the production capacity 100 MW at each end. Producer u_1 has the marginal cost 12 \$/MWh and producer u_2 has the marginal cost 11 \$/MWh. The transmission capacity of the line is $F = 130$ MW. A wind farm is connected to node 1 and it is scheduled to produce 70 MW. Demand is zero at node 1 and $D = 230$ MW at node 2. Both nodes are assumed to be in the same zone.

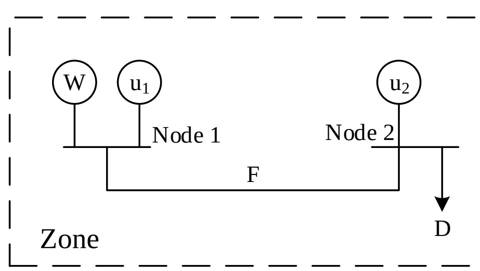

Figure 1: Single line diagram of 2-node example.

There are no shocks in this illustrative example. The system imbalance is zero in the real-time market, and the real-time market is only used for counter-trading. Thus, there is no trading in the real-time market unless the line is overloaded after the day-ahead market. Both nodes are in the same zone, so the transmission capacity is neglected in the day-ahead market. Producers use flat bids. Thus the line is overloaded by 40 MW if the bid price of producer u_1 is lower than the bid price of producer u_2, so that producer u_1 has the output 100 MW. The line is uncongested if producer u_1 has higher bid price than producer u_2, and then no trading is needed in the real-time market.

In case the line is overloaded after the day-ahead market, then producer u_1 is a buyer in the real-time market. At first we consider a UK design with pay-as-bid pricing in the real-time market. Assume that u_1 can make bids at 12 \$/MWh and \$10 \$/MWh. This is the only producer that can offer down-regulation in node 1. Thus it has monopoly power and therefore chooses to buy at the lowest price possible, i.e. 10 \$/MWh. Producer u_2 is a seller in the real-time market. Assume that it can make bids at 11 \$/MWh and 13 \$/MWh. This is the only producer that can offer up-regulation in node 2. Thus it has monopoly power and therefore chooses to sell at the highest price possible, i.e. 13 \$/MWh. Thus if the line is overloaded and all accepted bids are paid with their bid-price, then both producers make a profit of 80 \$/h in the real-time market. Otherwise there is no trade and no profit in the real-time market.

In the day-ahead market, we assume that producer u_1 can make bids at 10 \$/MWh, 12 \$/MWh or 14 \$/MWh and that producer u_2 can make bids at 11 \$/MWh or 13 \$/MWh. The example is constructed such that both bids are at least partly accepted in the day-ahead market. The highest bid sets the zonal price. The producer with the lowest bid sells 100 MW in the day-ahead market and the other producer sells 60 MW. If the line is overloaded after the zonal-clearing then both producers will gain 80 \$/h from the real-time market. Otherwise, they do not gain anything from the real-time market. Thus payoffs are as in Table 2-(a). From this payoff matrix, we can deduce that there are three SPNE (shown in bold fonts). Two of these SPNE are where the inc-dec game is played. In these cases, producer u_1 undercuts producer u_2 in the day-ahead market, which overloads the line. Next, it buys back power in the real-time market at a lower price. Producer u_2 sells power at 13 \$/MWh in both markets. There is also another SPNE where producer u_1 sets a high price 14 \$/MWh in the day-ahead market and producer u_2 sells its full capacity. In this equilibrium producer u_2 chooses a sufficiently low price, 11 \$/MWh, to ensure that producer u_1 will not find it profitable to deviate and undercut. This outcome does not congest the line, and there is no trading in the real-time market. The third equilibrium is related to the high-price equilibrium[4] that has been analyzed by von der Fehr and Harbord (1993) in single-stage electricity markets without network constraints.

In Approach 2, we will consider the case where the real-time market uses optimal zonal pricing. If the two nodes are in the same zone, this means that the real-time market will have the same price for both producers. The seller (up-regulator) has incentives to use its market power to increase its price, while the buyer (down-regulator) has incentives to decrease its price. The system operator sets a real-time price that no producers makes loss in the real-time market. If there is no such real-time price, then it will need to use a (socially) costly operation to make sure that there is one zonal real-time price. In our model, the system operator will spill wind to uphold this constraint, even if it makes production costs higher. Thus, the operator rejects the down-regulation of producer u_1, and instead orders a 40-MW spillage of wind production.

[4]In practice, the high-price equilibrium has been observed in the capacity market of New York State's electricity market, which is dominated by one supplier and where the demand variation is small, Schwenen (2015).

Table 2: Payoff tables of two-stage game in different real-time market designs

(a) Pay-as-bid

u_1 \ u_2	11 \$/MWh	13 \$/MWh
10 \$/MWh	(-20,80)	**(180,200)**
12 \$/MWh	(0,100)	**(180,200)**
14 \$/MWh	**(120,300)**	(120,300)

(b) Optimal zonal pricing

u_1 \ u_2	11 \$/MWh	13 \$/MWh
10 \$/MWh	(-100,80)	(100,200)
12 \$/MWh	(0,100)	(100,200)
14 \$/MWh	**(120,300)**	**(120,300)**

This will reduce the injection from node 1 and relieves the overloading in the transmission line. Producer u_2's up-regulation bid is accepted at 40 MW. In the equilibrium, producer u_2 makes the profit of 80 \$/h in the real-time market. Producer u_1 makes no profit. If the line is overloaded after the zonal-clearing then producer u_2 will gain 80 \$/h from the real-time market. Otherwise, they do not gain anything from the real-time market. Thus payoffs are as in Table 2-(b).

From this payoff matrix, we can deduce that there are two SPNE (shown in bold fonts). Both equilibria are related to the high-price equilibrium. This suggests that optimal zonal pricing in the real-time market can mitigate the inc-dec game (an arbitrage strategy), but also that the design does not seem to mitigate market power. We see that in the optimal zonal pricing the system operator needs to use costly alternatives, such as to spill wind power, to uphold the zonal price rule. But such outcomes will not be profitable for producers either, so in equilibrium they will choose bids that avoid such outcomes.

In our mathematical model, which is introduced in the next section, we will consider examples with demand shocks. This makes the mathematical model more realistic. Another advantage with this is that demand uncertainty will normally reduce the number of equilibria. For electricity markets without transmission constraints, it is well-known that the high-price equilibrium only exists for small demand shocks, see von der Fehr and Harbord (1993). This is also true in our example. Consider the high-price equilibrium where producer u_1 bids at 14 \$/MWh and producer u_2 makes a bid at 11 \$/MWh. It only makes sense for producer u_2 to make a bid at 11 \$/MWh, if the producer can be sure that this bid will never be price-setting. If the bid would be price-setting with a positive probability, then it is strictly better to increase the bid to 13 \$/MWh. But in that case, producer u_1 would find it profitable to undercut and to play the inc-dec game, i.e. the high-price equilibrium falls apart. This explains why empirical studies of electricity spot markets by Sioshansi and Oren (2007), Hortaçsu and Puller (2008), Wolak (2007), and experimental results by Brandts et al. (2014), find that bidding is inconsistent with the high-price equilibrium.

It is well-known that existence of pure-strategy equilibria can be problematic in price games with capacity constraints, especially if demand is uncertain. Our setting is different from von der Fehr and Harbord (1993), Blázquez de Paz (2018), and the classical Bertrand-Edgeworth game in that bid prices are chosen from a discrete set in our model. This makes it less profitable to undercut the competitor, and non-existence of pure-strategy equilibria is less of an issue. This is explored in more detail by Holmberg et al. (2013).

In the illustrative example, we characterized SPNE in a simple two-node network without any shocks. Next, we will consider more complicated networks with wind power shocks. In the next section, we formulate the mathematical model of such a two-stage game.

3. Mathematical Model

To find an equilibrium in a bidding game of a network with shocks is a large-scale and complex problem. Solving this problem by exploring an entire continuous solution space is normally not feasible, see Moiseeva and Hesamzadeh (2018). If one wants to explore all outcomes of such a game, and have control of all equilibria, then one needs to reduce the solution space by making the strategy set of bidders discrete as in Pereira et al. (2005), Barroso et al. (2006), Bakirtzis et al. (2007) and Hesamzadeh and Biggar (2012). Similar to these studies, we assume that each producer makes one bid per plant and chooses their bids from a discrete set of permissible prices. This is also related to how electricity markets are designed in practice, where a producer can make a finite number of bids per plant, see Anderson and Holmberg (2018), Holmberg and Wolak (2018). In particular, the electricity market in Colombia is such that a producer chooses one bid price per plant, see Wolak (2009). Moreover, similar to practice, see Holmberg et al. (2013), bid prices are chosen from a price grid, but in our model the grid is more coarse than in practice.

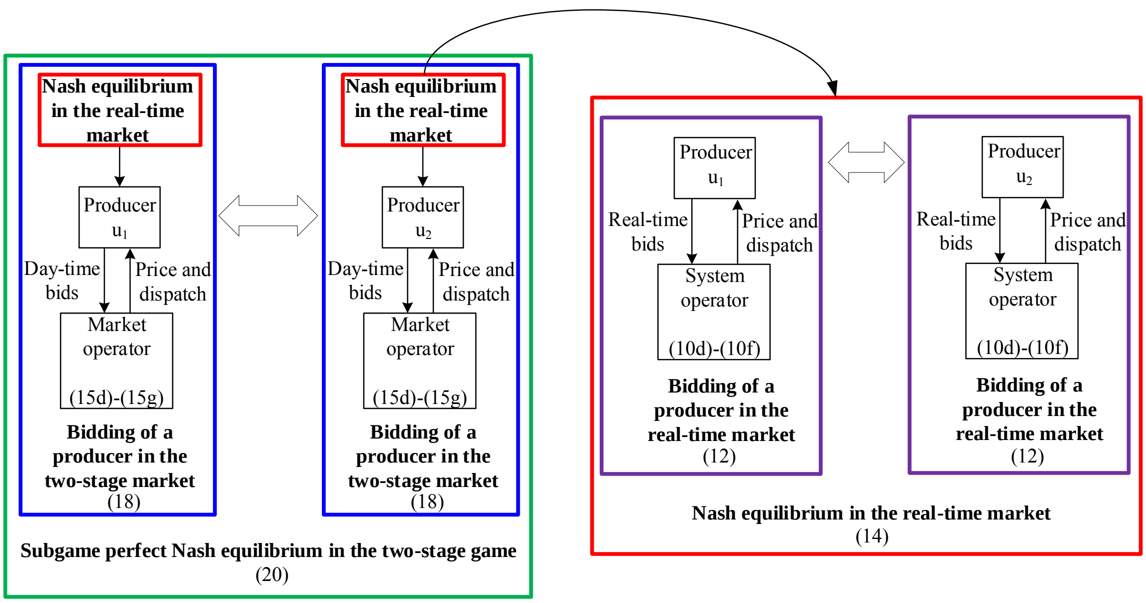

Figure 2: Structure of two-stage game, the numbers in parenthesis represents the mathematical models of each box.

In our model, each producer can choose a restricted number of prices which are related to the marginal cost of the producer. Each producer has unique costs and also a unique set of permissible prices. This means that there are no ties, and that we do not need a rationing rule. The structure of the two-stage game is illustrated in Fig. 2.

Each box in Fig. 2 represents different layers which we use to derive our mathematical model. First we start with formulating the economic dispatch model of each real-time pricing approach. Then, we formulate the bidding game of the producers in the real-time market, which constitutes the second stage of our two-stage game. Lastly, we add the first stage - the bidding game in the day-ahead market.

We consider a decentralized day-ahead market, which are normally used in Europe. Hence, retailers, wind-power owners, and large electricity consumers decide how much to buy/sell in the day-ahead market themselves. We assume that this volume is not perfectly predictable for the producers in our model. This gives a net-demand shock in the day-ahead market for them. The day-ahead prognosis of retailers etc. may not be correct, and this deviation gives another shock in the real-time market. Producers are assumed to have symmetric information. Hence, no producer makes a better, or worse, prognosis of net demand than any other producer in the model.

In Approach 2, we add a zonal constraint, which makes sure that nodal real-time prices are the same within a zone. It is not always feasible to maintain this constraint. Hence, we allow the system operator to spill wind in the real-time market to make it possible for the system operator to always find a feasible dispatch under the zonal constraint in our simulations.

3.1. Nomenclature

The main notation is presented below. Additional symbols are introduced throughout the text.

Indices

u	Producer, $u = 1, ..., U$
n	Power system node, $n = 1, ..., N$
i	Bidding strategy for real-time market, $i = 1, ..., I$
j	Bidding strategy for day-ahead market, $j = 1, ..., J$
z	Zone, $z = 1, ..., Z$
k	Transmission line, $k = 1, ..., K$
l	Inter-zonal line, $l = 1, ..., L$
m	Index of SPNE found, $m = 1, ..., M$
ω	Net demand scenario in day-ahead market, $\omega = 1, ..., \Omega$
s	Net demand deviation scenario in real-time market, $s = 1, ..., S$
a	Bidding action of producer, $a = 0, ..., A$

Parameters (upper-case letters)

$H_{k,n}$	PTDF matrix,
$H'_{l,z}$	Zonal PTDF matrix,
C_u	Marginal cost of unit u,
C_u^{up}	Marginal up-regulation cost of unit u,
C_u^{dn}	Marginal down-regulation cost of unit u,
G_u	Installed capacity of unit u,
F_k	Capacity of transmission line k,
$\bar{F}_l$	Capacity of inter-zonal line l,
$D_{n,\omega}$	Net demand at node n in scenario ω,
B_a	Step size of bidding action a,
B_a^{up}	Step size of up-regulation bidding action a,
B_a^{dn}	Step size of down-regulation bidding action a,
$\bar{W}_{n,\omega}$	Wind production at node n,
$\Delta W_{n,s\|\omega}$	Deviation in net demand at node n and scenario $s\|\omega$,
ξ_ω	Probability of scenario ω,
$\sigma_{s\|\omega}$	Conditional probability of scenario $s\|\omega$,
$\Psi_{u,n}$	Incidence matrix between u and n (1 if $u \in n$, 0 otherwise),
$\hat{\Psi}_{u,z}$	Incidence matrix between u and z (1 if $u \in z$, 0 otherwise),

$\tilde{\Psi}_{n,z}$	Incidence matrix between n and z (1 if $n \in z$, 0 otherwise),
Variables (lower-case letters)	
$t_{u,a}$	Binary variable of day-ahead bidding decision of unit u,
$t^{up}_{u,\omega,a}, (t^{dn}_{u,\omega,a})$	Binary variable for up-regulation (down-regulation) bidding decision of unit u,
$\hat{c}_u$	Price bid of unit u,
$\hat{c}^{up}_{u,\omega}, (\hat{c}^{dn}_{u,\omega})$	Up-regulation (down-regulation) price bid of unit u in scenario ω,
$g_{u,\omega}$	Production level of unit u in scenario ω,
$g^{up}_{u,s\|\omega}, (g^{dn}_{u,s\|\omega})$	Up (down) regulation provided by unit u in scenario $s\|\omega$,
$v_{n,s\|\omega}$	Wind spillage at node n in scenario $s\|\omega$,
$\rho_{n,s\|\omega}$	Real-time market price at node n in scenario $s\|\omega$,
$p_{n,\omega}$	Day-ahead market price at node n in scenario ω,
$\phi_{u,s\|\omega}$	Real-time profit of unit u in scenario $s\|\omega$,
$\pi_{u,\omega}$	Day-ahead profit of unit u in scenario ω.
$\phi^{(i),(j)}_{u,s\|\omega}$	Real-time profit of unit u for day-ahead strategy j and real-time strategy i,
$\pi^{(j)}_{u,\omega}$	Day-ahead profit of unit u for day-ahead strategy j.

3.2. Economic dispatch model in each real-time market approach

The system operator collects up-regulation and down-regulation bids from all producers and runs a bid-based economic dispatch to dispatch the regulation bids. In this section we formulate the economic-dispatch problem of each real-time pricing approach considered in this study.

3.2.1. Economic-dispatch model in Approach 1

Given regulation bids, $\hat{c}^{up}_{u,\omega}$ and $\hat{c}^{dn}_{u,\omega}$, the day-ahead shock ω, and the day-ahead dispatch, the economic dispatch in Approach 1 is formulated in (1).

$$\underset{g^{up}_{u,s|\omega}, g^{dn}_{u,s|\omega}, v_{n,s|\omega}}{\text{Minimize}} \quad \sum_{s|\omega} \sigma_{s|\omega} \sum_{u} (\hat{c}^{up}_{u,\omega} g^{up}_{u,s|\omega} - \hat{c}^{dn}_{u,\omega} g^{dn}_{u,s|\omega}) \tag{1a}$$

Subject to:

$$\sum_{u} (g_{u,\omega} + g^{up}_{u,s|\omega} - g^{dn}_{u,s|\omega}) = \sum_{n} (v_{n,s|\omega} + D_{n,\omega} - \Delta W_{n,s|\omega}) : (\alpha_{s|\omega}),\ \forall s|\omega \tag{1b}$$

$$F_k - \sum_{n} H_{k,n} (\sum_{u} \Psi_{u,n} (g_{u,\omega} + g^{up}_{u,s|\omega} - g^{dn}_{u,s|\omega}) - v_{n,s|\omega} - D_{n,\omega} + \Delta W_{n,s|\omega}) \geq 0 :$$
$$(\mu_{k,s|\omega}),\ \forall k, s|\omega \tag{1c}$$

$$0 \leq g^{up}_{u,s|\omega} \leq (G_u - g_{u,\omega}) : (\kappa_{u,s|\omega}, \beta_{u,s|\omega}),\ \forall u, s|\omega \tag{1d}$$

$$0 \leq g^{dn}_{u,s|\omega} \leq g_{u,\omega} : (\psi_{u,s|\omega}, \varphi_{u,s|\omega}),\ \forall u, s|\omega \tag{1e}$$

$$0 \leq v_{n,s|\omega} \leq \bar{W}_{n,\omega} + \Delta W_{n,s|\omega} : (\theta_{n,s|\omega}, \chi_{n,s|\omega}),\ \forall n, s|\omega \tag{1f}$$

The optimization problem (1) is a linear program (LP). $g_{u,\omega}$ is the given dispatch levels in the day-ahead market. The production cost in the real-time market is minimized in (1a) considering the energy balance constraint (1b), the transmission flow limits (1c), the capacity limits in (1d) and (1e) and the wind-spillage limit (1f). In (1c), parameter $\Psi_{u,n}$ is 1 if producer u is located at node n, otherwise it is zero. The Lagrange multipliers related to each constraint are given in parentheses.

In Approach 1, the producers are paid with their bid price in the real-time market. So the profit of producer u is formulated as in (2).

$$\phi_{u,s|\omega} = (\hat{c}^{up}_{u,\omega} - C^{up}_{u})g^{up}_{u,s|\omega} + (C^{dn}_{u} - \hat{c}^{dn}_{u,\omega})g^{dn}_{u,s|\omega} \tag{2}$$

3.2.2. Economic-dispatch model in Approach 2

In Approach 2, we consider a zonal real-time market where all accepted regulation bids are paid with the marginal zonal price. The system operator dispatches the regulation bids such that nodal prices in each zone are equal to each other and such that no producer makes a loss. A problem with this is that the economic dispatch is no longer a linear problem (LP)[5]. We need the lower level problem to be linear, so that we can replace it by its KKT conditions. Inspired by Ruiz et al. (2012), we deal with this by approximating the economic dispatch problem of the real-time market by formulating it as a primal-minus-dual model[6]. Another advantage with this approach is that we get access to the Lagrange variables (dual variables) of optimization problem (1).

Due to the zonal pricing constraint in (3a), the zonal price may not be set by the marginal producer but by a cheaper producer. This causes losses for the marginal producer. A market design which may result in losses for some producers may incentivize them to leave the market. To avoid this situation, we add constraint (3b) in the economic-dispatch problem in Approach 2. This is mathematically modeled by including constraint (3) to the economic-dispatch model.

$$\sum_{z} \tilde{\Psi}_{n,z}\rho'_{z,s|\omega} = \rho_{n,s|\omega}, \quad \forall n, s|\omega \tag{3a}$$

$$\phi_{u,s|\omega} \geq 0 \quad \forall u, s|\omega \tag{3b}$$

Terms $\rho'_{z,s|\omega}$, $\rho_{n,s|\omega}$ and $\phi_{u,s|\omega}$ represent the zonal real-time price, the nodal real-time price and the profit in the real-time market, respectively. In (3a), parameter $\tilde{\Psi}_{n,z}$ is 1 if node n is located at zone z, otherwise it is zero. The nodal real-time price is calculated as in (4).

$$\rho_{n,s|\omega} = (\alpha_{s|\omega} - \sum_{k} H_{k,n}\mu_{k,s|\omega})/\sigma_{s|\omega} \tag{4}$$

The profit of producer u in Approach 2 is formulated in (5). Here parameter $\hat{\Psi}_{u,z}$ is 1 if producer u is located at zone z, otherwise it is zero.

$$\phi_{u,s|\omega} = (\sum_{z} \hat{\Psi}_{u,z}\rho'_{z,s|\omega} - C^{up}_{u})g^{up}_{u,s|\omega} + (C^{dn}_{u} - \sum_{z} \hat{\Psi}_{u,z}\rho'_{z,s|\omega})g^{dn}_{u,s|\omega} \tag{5}$$

To formulate the primal-minus-dual model, we take LP problem (1) as our primal problem

[5]The economic dispatch problem is non-linear in Bjørndal and Jørnsten (2001) and Bjørndal et al. (2012), who simulate optimal zonal pricing for day-ahead markets. In our setting, the economic dispatch problem of the real-time market could be formulated as a MILP, but it is still not an LP.

[6]In Ruiz et al. (2012), the nonlinearity due to the market clearing price being multiplied by the dispatch quantity in the profit function is tackled by applying a discrete approximation, whereby the problem is transformed into a MILP model. In this study, we instead linearize the nonlinearity by using the stationary conditions (6c) and (6d) and the complimentary slackness conditions for (1d) and (1e). This approach results in an LP model. Similar approaches are for example used by Hesamzadeh and Biggar (2012) and Hesamzadeh and Biggar (2013). The approximation error due to the linearization is small as long as the duality gap is small.

and we derive the dual LP problem associated with the primal problem. Then we formulate a new LP problem which minimizes the duality gap of the primal and dual problems subject to both primal and dual constraints. Including the constraints (3) into the primal minus dual model which gives us the economic dispatch model of Approach 2. This is set out in (6).

$$\underset{\Pi}{\text{Minimize}} \quad \sum_{s|\omega} \sigma_{s|\omega} \sum_{u} (\hat{c}^{up}_{u,\omega} g^{up}_{u,s|\omega} - \hat{c}^{dn}_{u,\omega} g^{dn}_{u,s|\omega}) + \sum_{s|\omega} (\alpha_{s|\omega} (\sum_{u} g_{u,\omega} - \sum_{n} (D_{n,\omega} - \Delta W_{n,s|\omega})) + \sum_{k} \mu_{k,s|\omega} (F_k - \sum_{n} H_{k,n} (\sum_{u} \Psi_{u,n} g_{u,\omega} - D_{n,\omega} + \Delta W_{n,s|\omega})) + \sum_{u} (\beta_{u,s|\omega} (G_u - g_{u,\omega}) + \varphi_{u,s|\omega} g_{u,\omega}) + \sum_{n} \chi_{n,s|\omega} (W_{n,\omega} + \Delta W_{n,s|\omega})) \quad (6a)$$

Subject to:

$$\text{Constraints } (1b) - (1f) : (\lambda^A_{s|\omega}, \lambda^B_{k,s|\omega}, \lambda^C_{u,s|\omega}, \lambda^D_{u,s|\omega}, \lambda^E_{u,s|\omega}, \lambda^F_{u,s|\omega}, \lambda^G_{n,s|\omega}, \lambda^H_{n,s|\omega}) \quad (6b)$$

$$-\sigma_{s|\omega} \hat{c}^{up}_{u,\omega} + \alpha_{s|\omega} - \sum_{n} \Psi_{u,n} \sum_{k} H_{k,n} \mu_{k,s|\omega} + \kappa_{u,s|\omega} - \beta_{u,s|\omega} = 0 : (\lambda^I_{u,s|\omega}),\ \forall u, s|\omega \quad (6c)$$

$$\sigma_{s|\omega} \hat{c}^{dn}_{u,\omega} - \alpha_{s|\omega} + \sum_{n} \Psi_{u,n} \sum_{k} H_{k,n} \mu_{k,s|\omega} + \psi_{u,s|\omega} - \varphi_{u,s|\omega} = 0 : (\lambda^J_{u,s|\omega}),\ \forall u, s|\omega \quad (6d)$$

$$-\alpha_{s|\omega} + \sum_{k} H_{k,n} \mu_{k,s|\omega} + \theta_{n,s|\omega} - \chi_{n,s|\omega} = 0 : (\lambda^K_{n,s|\omega}),\ \forall n, s|\omega \quad (6e)$$

$$\mu_{k,s|\omega}, \kappa_{u,s|\omega}, \beta_{u,s|\omega}, \psi_{u,s|\omega}, \varphi_{u,s|\omega}, \theta_{n,s|\omega}, \chi_{n,s|\omega} \geq 0 : (\lambda^N_{k,s|\omega}, \lambda^O_{u,s|\omega}, \lambda^P_{u,s|\omega}, \lambda^Q_{u,s|\omega}, \lambda^R_{u,s|\omega}, \lambda^S_{n,s|\omega}, \lambda^T_{n,s|\omega}) \quad (6f)$$

$$\sum_{z} \hat{\Psi}_{n,z} \rho'_{z,s|\omega} = (\alpha_{s|\omega} - \sum_{k} H_{k,n} \mu_{k,s|\omega}) / \sigma_{s|\omega} : (\lambda^L_{n,s|\omega}), \forall n, s|\omega \quad (6g)$$

$$\phi_{u,s|\omega} \geq 0 : (\lambda^M_{u,s|\omega}), \forall u, s|\omega \quad (6h)$$

$$\phi_{u,s|\omega} = (\beta_{u,s|\omega} (G_u - g_{u,\omega}) + \varphi_{u,s|\omega} g_{u,\omega}) / \sigma_{s|\omega} + C^{dn}_u g^{dn}_{u,s|\omega} - \hat{c}^{dn}_{u,\omega} g^{dn}_{u,s|\omega} + \hat{c}^{up}_{u,\omega} g^{up}_{u,s|\omega} - C^{up}_u g^{up}_{u,s|\omega}, \quad \forall u, s|\omega \quad (6i)$$

The set of decision variables in (6) is $\Pi = \{g^{up}_{u,s|\omega},\ g^{dn}_{u,s|\omega},\ v_{n,s|\omega},\ \alpha_{s|\omega},\ \mu_{k,s|\omega},\ \kappa_{u,s|\omega},\ \beta_{u,s|\omega},\ \psi_{u,s|\omega},\ \varphi_{u,s|\omega},\ \theta_{n,s|\omega},\ \chi_{n,s|\omega},\ \rho'_{z,s|\omega},\ \phi_{u,s|\omega}\}$. Constraint (6b) is from the primal problem of (1) and constraints (6c)-(6f) are from the dual problem of (1). Additional constraints for zonal real-time market in (3) is given in (6g) and (6h) in the context of optimization problem (6). The profit function in (5) is reformulated using (6c) and (6d) and the complementary slackness conditions for (1d)-(1e) in (6i). Optimization problem (6) is a LP model. The Lagrange multipliers related to each constraint are given in parentheses.

Note that primal minus dual model (6a)-(6f) is a relaxation of (1). The gap due to the relaxation is measured by the duality gap expression which is minimized in (6a). If the duality gap is equal to zero, then the optimal solutions of (1) and (6a)-(6f) are equivalent. Otherwise, the solution of (6a)-(6f) is as close as possible to that of (1), since the feasible region of (6a)-(6f) is built around the optimal solution of (1), see Ruiz et al. (2012).

The economic dispatch problems in the real-time market in Approach 1 and Approach 2 are formulated as LPs in (1) and (6), respectively. The Lagrange multipliers related to each constraint are given in parentheses. To keep our model derivations concise, we will illustrate them in general matrix form as in (7).

$$\underset{\boldsymbol{x}}{\text{Minimize}} \;\; \boldsymbol{C}^T\boldsymbol{x} \tag{7a}$$

Subject to:

$$\boldsymbol{Ax} + \boldsymbol{Bxg} + \boldsymbol{Dg} + \boldsymbol{E} = 0: \;\; (\boldsymbol{\lambda}) \tag{7b}$$

$$\boldsymbol{Fx} + \boldsymbol{Gxg} + \boldsymbol{Hg} + \boldsymbol{I} \geq 0: \;\; (\boldsymbol{\mu}) \tag{7c}$$

Here vector $\boldsymbol{x}$ represents all decision variables in (1) or (6). Matrices $\boldsymbol{A}$, $\boldsymbol{B}$, $\boldsymbol{D}$, $\boldsymbol{E}$, $\boldsymbol{F}$, $\boldsymbol{G}$, $\boldsymbol{H}$ and $\boldsymbol{I}$ are the coefficient matrices. Term $\boldsymbol{C}^T$ is the transpose of vector $\boldsymbol{C}$. Vector $\boldsymbol{g}$ represents the day-ahead dispatch decisions which are given parameters in (7). It is shown separately for facilitating further derivation of our two-stage game model.

3.3. Bidding game in the real-time market

We want to solve for a SPNE in the two-stage game. Thus whatever happened in the first-stage, producers will be sequentially rational and play a Nash equilibrium in the second stage. It is most straightforward to solve for a SPNE backwards, so we start with the last stage, the real-time market.

3.3.1. Single producer's bidding problem in the real-time market

Each producer submits its up-regulation and down-regulation bids to the real-time market given the dispatch results in the day-ahead market. Moreover, we solve for a Nash equilibrium in the real-time market, so each producer chooses a bid that is a best response to the bids of its rivals in the real-time market. This is illustrated in the purple box in Fig. 2. The strategic bidding decision of producer u in the real-time market is formulated as a two-stage stochastic bilevel optimization problem in (8).

$$\underset{\hat{c}^{up}_{u,\omega},\hat{c}^{dn}_{u,\omega},t^{up}_{u,\omega,a},t^{dn}_{u,\omega,a}}{\text{Maximize}} \quad \mathbb{E}_{s|\omega}[\phi_{u,s|\omega}] \tag{8a}$$

Subject to:

$$\hat{c}^{up}_{u,\omega} = \sum_a B^{up}_a t^{up}_{u,\omega,a} C^{up}_u, \quad \hat{c}^{dn}_{u,\omega} = \sum_a B^{dn}_a t^{dn}_{u,\omega,a} C^{dn}_u \tag{8b}$$

$$t^{up}_{u,\omega,a}, t^{dn}_{u,\omega,a} \in \{0,1\} \tag{8c}$$

$$\sum_a t^{up}_{u,\omega,a} = 1, \quad \sum_a t^{dn}_{u,\omega,a} = 1 \tag{8d}$$

$$\text{where}\{\boldsymbol{x}\} \in \Bigg\{ \underset{\boldsymbol{x}}{\text{argMinimize}} \;\; \boldsymbol{C}^T\boldsymbol{x} \tag{8e}$$

Subject to:

$$\boldsymbol{Ax} + \boldsymbol{Bxg} + \boldsymbol{Dg} + \boldsymbol{E} = 0: \;\; (\boldsymbol{\lambda}) \tag{8f}$$

$$\boldsymbol{Fx} + \boldsymbol{Gxg} + \boldsymbol{Hg} + \boldsymbol{I} \geq 0: \;\; (\boldsymbol{\mu}) \Bigg\} \tag{8g}$$

Objective function (8a) maximizes the expected profit in the real-time market. The up-regulation and the down-regulation price bids are modeled using binary variables $t^{up}_{u,\omega,a}$ and $t^{dn}_{u,\omega,a}$ in (8b). Here parameters B^{up}_a and B^{dn}_a represent the mark-up and mark-down options in bidding action a, respectively. Constraint (8d) ensures that only one bidding action is selected. Optimization problem (8e)-(8g) formulates the economic dispatch problem in the real-time market. The Lagrange multipliers related to constraints (8f)-(8g) are given in parentheses. Optimization problem (8) is a bilevel optimization problem. The most straightforward way to solve a bilevel optimization problem is to replace the inner optimization problem by its Karush-Kuhn-Tucker (KKT) conditions. This approach transforms the bilevel optimization problem into a single level optimization problem. Since (8e)-(8g) is LP, the KKT conditions are both necessary and sufficient for a best response, which is shown by Gabriel et al. (2012). The bilinear complementary slackness conditions[7] are replaced by the strong duality conditions. This replacement enables us to reduce the number of the constraints and the bilinear terms. This is explained in further detail in Appendix A. The stationary, dual feasibility and strong duality conditions of (8e)-(8g) are presented in (10g), (10h) and (10i), respectively.

The stationary, dual feasibility and strong duality conditions related to the economic dispatch problems in Approach 1 and Approach 2 are explicitly presented in Appendix B. Bidding decisions $\hat{c}^{up}_{u,\omega}$ and $\hat{c}^{dn}_{u,\omega}$ are defined using binary variables $t^{up}_{u,\omega,a}$ and $t^{dn}_{u,\omega,a}$ in (8b). After replacing (8e)-(8g) with its KKT conditions, we face bilinear terms $\boldsymbol{x}t^{up}_{u,\omega,a}$ and $\boldsymbol{x}t^{dn}_{u,\omega,a}$ in the resulting single-level optimization problem. These bilinear terms consist of the binary variables related to the bidding decisions, $t^{up}_{u,\omega,a}$ and $t^{up}_{u,\omega,a}$, and the continuous variables, $\boldsymbol{x}$, from the KKT conditions of the economic dispatch problem. The detailed list of bilinear terms and their locations are illustrated in Table 3.

Table 3: Bilinear terms linearized in (10) in each real-time pricing approach

	Approach 1	Approach 2
$t^{up}_{u,\omega,a}g^{up}_{u,s\|\omega}$	in (2) and (B.1e)	in (6i) and (B.2n)
$t^{dn}_{u,\omega,a}g^{dn}_{u,s\|\omega}$	in (2) and (B.1e)	in (6i) and (B.2n)
$t^{up}_{u,\omega,a}\lambda^{M}_{u,s\|\omega}$	-	in (B.2a)
$t^{dn}_{u,\omega,a}\lambda^{M}_{u,s\|\omega}$	-	in (B.2b)
$t^{up}_{u,\omega,a}\lambda^{I}_{u,s\|\omega}$	-	in (B.2n)
$t^{dn}_{u,\omega,a}\lambda^{J}_{u,s\|\omega}$	-	in (B.2n)

These bilinear terms are linearized using the McCormick reformulation, see Gupte et al. (2013). The McCormick reformulation is a technique for linearizing the bilinear terms which consists of the product of a binary and a continuous variable. To explain the method, assume that we want to linearize $t^{up}_{u,\omega,a}g^{up}_{u,s|\omega}$, one of the bilinear terms in Table 3. We first replace the bilinear term with a new variable $\tau_{u,a,s|\omega} = t^{up}_{u,\omega,a}g^{up}_{u,s|\omega}$ and then add the following linear constraints.

$$g^{up}_{u,s|\omega} + G_u(t^{up}_{u,\omega,a} - 1) \leq \tau_{u,a,s|\omega} \leq g^{up}_{u,s|\omega} \tag{9a}$$

$$0 \leq \tau_{u,a,s|\omega} \leq G_u t^{up}_{u,\omega,a} \tag{9b}$$

We used the nodal pricing regime as a benchmark in our study. We model it as a zonal system with one node per zone so the profit function of the benchmark model is (5).

Now we can formulate the MILP model of each producer's bidding problem in the real-time market as in (10).

[7]The complementary slackness conditions are given by the product of inequality constraints and their related Lagrange multipliers should be equal to zero. This is bilinear due to the product of two continuous variables. The number of bilinear terms increases with the number of the inequality constraints.

$$\underset{\Theta}{\text{Maximize}} \quad \mathbb{E}_{s|\omega}[\phi_{u,s|\omega}] \tag{10a}$$

Subject to:

$$\hat{c}^{up}_{u,\omega} = \sum_a B^{up}_a t^{up}_{u,\omega,a} C^{up}_u, \ \hat{c}^{dn}_{u,\omega} = \sum_a B^{dn}_a t^{dn}_{u,\omega,a} C^{dn}_u \tag{10b}$$

$$t^{up}_{u,\omega,a}, t^{dn}_{u,\omega,a} \in \{0,1\} \tag{10c}$$

$$\sum_a t^{up}_{u,\omega,a} = 1, \quad \sum_a t^{dn}_{u,\omega,a} = 1 \tag{10d}$$

$$\boldsymbol{Ax} + \boldsymbol{Bxg} + \boldsymbol{Dg} + \boldsymbol{E} = 0 \tag{10e}$$

$$\boldsymbol{Fx} + \boldsymbol{Gxg} + \boldsymbol{Hg} + \boldsymbol{I} \geq 0 \tag{10f}$$

$$-\boldsymbol{C} + \boldsymbol{\lambda}(\boldsymbol{A}^T + \boldsymbol{B}^T\boldsymbol{g}^T) + \boldsymbol{\mu}(\boldsymbol{F}^T + \boldsymbol{G}^T\boldsymbol{g}^T) = 0 \tag{10g}$$

$$\boldsymbol{\mu} \geq 0 \tag{10h}$$

$$-\boldsymbol{C}^T\boldsymbol{x} - (\boldsymbol{\lambda}(\boldsymbol{E}^T + \boldsymbol{D}^T\boldsymbol{g}^T) + \boldsymbol{\mu}(\boldsymbol{I}^T + \boldsymbol{H}^T\boldsymbol{g}^T)) = 0 \tag{10i}$$

$$\text{Linearization of bilinear terms in Table 3 as in (9)} \tag{10j}$$

The set of decision variables in (10) is $\Theta = \{\hat{c}^{up}_{u,\omega},\ \hat{c}^{dn}_{u,\omega},\ t^{up}_{u,\omega,a},\ t^{dn}_{u,\omega,a},\ \phi_{u,s|\omega},\ \boldsymbol{x},\ \boldsymbol{\lambda},\ \boldsymbol{\mu}\}$.

3.3.2. Nash equilibrium in the real-time market

The red box in Fig. 2 illustrates the Nash equilibrium in the real-time market. The Nash equilibrium in the real-time market given the day-ahead dispatch decisions is found by solving all producers' bidding problems in the real-time market simultaneously. Since price bids $\hat{c}^{up}_{u,\omega}$ and $\hat{c}^{dn}_{u,\omega}$ are chosen from a discrete set, each producer's alternative strategies $\{\hat{c}^{up,(1)}_{u,\omega},\ \hat{c}^{dn,(1)}_{u,\omega},\ \hat{c}^{up,(2)}_{u,\omega},\ \hat{c}^{dn,(2)}_{u,\omega},...,\hat{c}^{up,(I)}_{u,\omega},\ \hat{c}^{dn,(I)}_{u,\omega}\}$ can be formed by different combinations of binary variables $t^{up}_{u,\omega,a}$ and $t^{dn}_{u,\omega,a}$. The real-time profit of each producer in these alternative strategies can be calculated by MILP model (10) while holding its rivals' strategies fixed. Hence, we can reformulate MILP model (10) of each producer as a set of Mixed-Integer Linear Constraints (MILC) by replacing objective function (10a) by constraint (11). In (11), $\mathbb{E}_{s|\omega}[\phi_{u,s|\omega}]$ and $\mathbb{E}_{s|\omega}[\phi^{(i)}_{u,s|\omega}]$ represent the real-time profit of producer u in the Nash equilibrium strategy and in alternative strategy i, respectively.

$$\mathbb{E}_{s|\omega}[\phi_{u,s|\omega}] \geq \mathbb{E}_{s|\omega}[\phi^{(i)}_{u,s|\omega}], \quad \forall i \tag{11}$$

The Nash equilibrium in the real-time market is found by solving all the MILCs of all producers simultaneously[8]. This is formulated as a feasibility problem in (12).

$$RTNE_\omega = \Big\{ \text{Find} \quad \Theta \cup \Theta^{(i)}, \quad \forall u \tag{12a}$$

$$\text{Such that}$$

$$\text{Constraints } (10b) - (10j), \quad \forall u \tag{12b}$$

$$\text{Constraints } (10b)^{(i)} - (10j)^{(i)} \quad \forall u, i \tag{12c}$$

$$\mathbb{E}_{s|\omega}[\phi_{u,s|\omega}] \geq \mathbb{E}_{s|\omega}[\phi^{(i)}_{u,s|\omega}], \quad \forall u, i \Big\} \tag{12d}$$

[8]It might seem that an alternative way of solving this is to take the KKT conditions of each producer's bidding problem (10) and to solve them together. However, in our model, optimization problem (10) is MILP. Hence the KKT conditions of (10) are not necessary and sufficient. That's why we cannot use this method to model the Nash equilibrium in the real-time market.

Here Θ is the set of decision variables related to the bidding problem of producer u for the Nash equilibrium strategy and $\Theta^{(i)}$ is the set of decision variables related to producer u in alternative strategy i given the strategies of its rivals. Constraints (12b) and (12c) are written for the Nash equilibrium strategy and for the alternative strategy i, respectively. Constraint (12d) ensures for all producers that the real-time profit in the Nash equilibrium strategy is greater or equal than the one in all alternative strategies. A feasible solution of (12) is the Nash equilibrium in the real-time market, $RTNE_{\omega}$.

3.4. Bidding game in the day-ahead market

In the day-ahead market, the producers choose their day-ahead bids from a discrete set of permissible prices. Similar to the real-time market, each producer has a unique set of permissible price bids. We consider cases where the market operator has set the flow limits between the zones for the day-ahead dispatch at a level which ensures security of the power system.

3.4.1. Single producer's bidding problem in the day-ahead market

We solve for a SPNE. Thus, producer u submits an optimal bid to the day-ahead market given the day-ahead bids of its rivals and considering the resulting Nash equilibrium in the real-time market. This is illustrated in the blue box in Fig. 2 and formulated in (13).

$$\underset{\Lambda}{\text{Maximize}} \quad \mathbb{E}_{\omega}[(\sum_{z}\hat{\Psi}_{u,z}p_{z,\omega} - C_u)g_{u,\omega} + \mathbb{E}_{s|\omega}[\phi_{u,s|\omega}]] \tag{13a}$$

Subject to:

$$\hat{c}_u = \sum_{a} B_a t_{u,a} C_u, \ \forall u \tag{13b}$$

$$t_{u,a} \in \{0,1\} \tag{13c}$$

$$\sum_{a} t_{u,\omega,a} = 1 \tag{13d}$$

$$RTNE_{\omega} \ \forall\omega \tag{13e}$$

$$\text{where}\{p_{u,\omega}, g_{u,\omega}\} \in \Bigg\{ \underset{g_{u,\omega}}{\text{argMinimize}} \quad \sum_{u,\omega}\xi_{\omega}(\hat{c}_u g_{u,\omega}) \tag{13f}$$

Subject to:

$$\sum_{u} g_{u,\omega} = \sum_{n} D_{n,\omega} \ : (\delta_{\omega}) \ \forall\omega \tag{13g}$$

$$\bar{F}_l - \sum_{z} H'_{l,z}(\sum_{u}\hat{\Psi}_{u,z}g_{u,\omega} - \sum_{n}\tilde{\Psi}_{n,z}D_{n,\omega}) \geq 0 \ : (\gamma_{l,\omega}) \ \forall l,\omega \tag{13h}$$

$$0 \leq g_{u,\omega} \leq G_u \ : (\eta_{u,\omega}, \nu_{u,\omega}) \ \forall u,\omega \Bigg\} \tag{13i}$$

The set of decision variables in (13) is $\Lambda = \{\hat{c}_u, \ t_{u,a},\} \cup \Theta \cup \Theta^{(i)}$. Objective function (13a) maximizes the total expected profit in the day-ahead and the real-time markets. Equation (13b) models the price bids that producer u submitted to the day-ahead market. Constraint (13d) ensures that only one bidding action is selected. Optimization problem (13f)-(13i) formulates the economic dispatch problem in the day-ahead market. The total stated production cost is minimized in (13f) (by the market operator) considering the energy balance constraint (13g), the inter-zonal transmission limits (13h) and generation limits (13i). The Lagrange multipliers related to each constraint are given in parentheses. We transform bilevel optimization problem (13) to a single-level optimization problem by replacing inner optimization problem (13f)-(13i) by its KKT conditions. Since problem (13f)-(13i) is a linear program, its KKT conditions are necessary and sufficient.

The profit in the day-ahead market is formulated as $\pi_{u,\omega} = (\sum_z \hat{\Psi}_{u,z} p_{z,\omega} - C_u) g_{u,\omega}$. Here $p_{z,\omega}$ is the zonal price in the day-ahead market which can be calculated as $p_{z,\omega} = \delta_\omega - \sum_l H'_{l,z} \gamma_{l,\omega}$. The day-ahead profit can be reformulated in (14) using the stationary condition (shown in (16h)) and the complementary slackness conditions for (13i).

$$\pi_{u,\omega} = \nu_{u,\omega} G_u + (\hat{c}_u - C_u) g_{u,\omega}, \ \forall u, \omega \tag{14}$$

After replacing (13f)-(13i) by its KKT conditions, two types of bilinear terms appear in the resulting model. The first type consists of the product of the binary variable from day-ahead bidding decision and the day-ahead dispatch ($t_{u,a} g_{u,\omega}$). These bilinear terms are linearized using the McCormick reformulation. The second type consists of continuous variables from the KKT conditions of real-time market models and the day-ahead dispatch quantity, $\boldsymbol{xg}$, $\boldsymbol{\lambda g}$ and $\boldsymbol{\mu g}$. The detailed list of the bilinear terms and their locations are presented in Table 4. It follows from the lemma below that also the second type of bilinear terms can be linearized by the McCormick reformulation.

Table 4: Bilinear terms linearized in (16) in each real-time pricing approach

Bilinear term	Approach 1	Approach 2
$\alpha_{s\|\omega} \sum_u g_{u,\omega}$	in (B.1e)	in (B.2n)
$\mu_{k,s\|\omega} \sum_n H_{k,n} \sum_{u:n} g_{u,\omega}$	in (B.1e)	in (B.2n)
$\beta_{u,s\|\omega} g_{u,\omega}$	in (B.1e)	in (6i) and (B.2n)
$\varphi_{u,s\|\omega} g_{u,\omega}$	in (B.1e)	in (6i) and (B.2n)
$\lambda^M_{u,s\|\omega} g_{u,\omega}$	-	in (B.2h) and (B.2j)
$\lambda^A_{s\|\omega} \sum_u g_{u,\omega}$	-	in (B.2n)
$\lambda^B_{k,s\|\omega} \sum_n H_{k,n} \sum_{u:n} g_{u,\omega}$	-	in (B.2n)
$\lambda^D_{u,s\|\omega} g_{u,\omega}$	-	in (B.2n)
$\lambda^F_{u,s\|\omega} g_{u,\omega}$	-	in (B.2n)

Lemma 1
Day-ahead dispatch quantity $g_{u,\omega}$ is a discrete variable.

Proof. Since the following three conditions are satisfied in day-ahead economic dispatch model (13f)-(13i): (i) the net-demand at each node in each scenario is fixed and given, (ii) the capacities of each unit and each inter-zonal line are given and (iii) the price bids are flat and they are chosen from a unique and finite set of discrete values, the corresponding dispatch interactions are also chosen from a finite set of discrete values[9]. □

[9]This lemma means that the day-ahead economic dispatch model is originally a discretely-constrained LP model.The LP model we assumed for deriving the KKT conditions is the relaxation of the discretely-constrained LP model with zero duality gap.

We mathematically model $g_{u,\omega}$ as discrete variable by introducing binary variable $y_{u,\omega,r}$ in (15).

$$g_{u,\omega} = \sum_r E_{u,\omega,r} y_{u,\omega,r},\ \forall u, \omega, \quad \sum_r y_{u,\omega,r} \leq 1,\ \forall u, \omega \quad \text{and} \quad y_{u,\omega,r} \in \{0,1\},\ \forall u, \omega, r \qquad (15)$$

In (15), $E_{u,\omega,r}$ is a parameter which is the day-ahead dispatch of producer u in bid combination r. Let's assume we have U producers in the day-ahead market and each producer has A bid alternatives, then we have A^U bid combinations. Here we define index r as $r = 1, ..., A^U$. Parameter $E_{u,\omega,r}$ is calculated by solving (13f)-(13i) for all A^U bid combinations. Each bid combination is independent from each other, therefore this calculation can be done using parallel computing.

Now, we can formulate the MILP model of each producer's bidding problem in two-stage markets as in (16).

$$\underset{\Gamma}{\text{Maximize}} \qquad \mathbb{E}_\omega[(\sum_z \hat{\Psi}_{u,z} p_{z,\omega} - C_u) g_{u,\omega} + \mathbb{E}_{s|\omega}[\phi_{u,s|\omega}]] \qquad (16a)$$

Subject to:

$$\hat{c}_u = \sum_a B_a t_{u,a} C_u,\ \forall u \qquad (16b)$$

$$t_{u,a} \in \{0,1\} \qquad (16c)$$

$$\sum_a t_{u,a} = 1 \qquad (16d)$$

$$\sum_u g_{u,\omega} = \sum_n D_{n,\omega}, \quad \forall \omega \qquad (16e)$$

$$\bar{F}_l - \sum_z H'_{l,z} (\sum_u \hat{\Psi}_{u,z} g_{u,\omega} - \sum_n \tilde{\Psi}_{n,z} D_{n,\omega}) \geq 0, \quad \forall l, \omega \qquad (16f)$$

$$0 \leq g_{u,\omega} \leq G_u, \quad \forall u, \omega \qquad (16g)$$

$$-\xi_\omega \hat{c}_u + \delta_\omega - \sum_z \hat{\Psi}_{u,z} \sum_l H'_{l,z} \gamma_l + \eta_{u,\omega} - \nu_{u,\omega} = 0,\ \forall u, \omega \qquad (16h)$$

$$\gamma_{l,\omega}, \eta_{u,\omega}, \nu_{u,\omega} \geq 0 \qquad (16i)$$

$$-\sum_u \xi_\omega \hat{c}_u g_{u,\omega} - (\delta_\omega \sum_n -D_{n,\omega} + \sum_l \gamma_{l,\omega} (\bar{F}_l - \sum_z H'_{l,z} (\sum_n -\Psi_{n,z} D_{n,\omega})) +$$
$$\sum_u \nu_{u,\omega} G_u = 0, \quad \forall \omega \qquad (16j)$$

$$g_{u,\omega} = \sum_r E_{u,\omega,r} y_{u,\omega,r}, \quad \forall u, \omega \qquad (16k)$$

$$\sum_r y_{u,\omega,r} \leq 1, \quad \forall u, \omega \qquad (16l)$$

Linearization of bilinear terms in Table 4 as in (9) (16m)

$RTNE_\omega, \quad \forall \omega$ (16n)

The set of decision variables in (16) is $\Gamma = \{g_{u,\omega},\ \delta_\omega,\ \gamma_{l,\omega},\ \eta_{u,\omega},\ \nu_{u,\omega},\ p_{z,\omega},\ y_{u,\omega,r}\} \cup \Lambda$.

3.4.2. Subgame Perfect NE in the two-stage game

The SPNE is found by solving MILP model (16) of all producers simultaneously as illustrated in the green box in Fig. 2. Analogous to the modeling of the Nash equilibrium in the real-time market, we reformulate MILP model (16) of each producer as a set of MILC by replacing objective function (16a) by constraint (17). In (17), $\mathbb{E}_{\omega}[\pi_{u,\omega} + \mathbb{E}_{s|\omega}[\phi_{u,s|\omega}]]$ and $\mathbb{E}_{\omega}[\pi^{(j)}_{u,\omega} + \mathbb{E}_{s|\omega}[\phi^{(i),(j)}_{u,s|\omega}]]$ represent the total expected profit of producer u in the SPNE and in alternative strategies i and j, respectively.

$$\mathbb{E}_{\omega}[\pi_{u,\omega} + \mathbb{E}_{s|\omega}[\phi_{u,s|\omega}]] \geq \mathbb{E}_{\omega}[\pi^{(j)}_{u,\omega} + \mathbb{E}_{s|\omega}[\phi^{(i),(j)}_{u,s|\omega}]] \ \forall u, i, j \tag{17}$$

Solving the MILCs of all producers simultaneously gives us the SPNE of the two-stage game. This is formulated by feasibility problem (18).

$$\text{Find} \quad \Gamma \cup \Gamma^{(j)} \tag{18a}$$

$$\text{Such that}$$

$$\text{Constraints } (16b) - (16n) \tag{18b}$$

$$\text{Constraints } (16b)^{(j)} - (16n)^{(j)}, \quad \forall j \tag{18c}$$

$$\mathbb{E}_{\omega}[\pi_{u,\omega} + \mathbb{E}_{s|\omega}[\phi_{u,s|\omega}]] \geq \mathbb{E}_{\omega}[\pi^{(j)}_{u,\omega} + \mathbb{E}_{s|\omega}[\phi^{(i),(j)}_{u,s|\omega}]] \ \forall u, i, j \tag{18d}$$

Our benchmark model is the nodal pricing model. Mathematically, the only difference to the zonal day-ahead model is that constraint (16f) is replaced by the constraint $(F_k - \sum_n H_{k,n}(\sum_u \Psi_{u,n} g_{u,\omega} - D_{n,\omega}) \geq 0)$.

4. Tackling Multiple SPNE

The number of producers and the number of strategies available for each producer influences the existence and the number of SPNE. In case of multiple SPNE, the market outcomes may differ between different SPNE, which would complicate the market analysis. This study uses two methodologies to tackle the multiple SPNE.

4.1. Methodology 1: Finding all SPNE

To find all SPNE, we develop an iterative procedure. Once a SPNE is found, an integer cut is included in MILC model (18) and the new resulting MILC model (MILC model (18) and the integer cut of the previous SPNE) is solved for a new SPNE. The function of the integer cut is to exclude the previous SPNE (values of binary variables) from the feasibility region. This process continues until the resulting MILC model has no feasible solution.

Constraint (19) formulates the integer cut in iteration m. Vector $\boldsymbol{h}$ consists of all binary variables $\boldsymbol{h} = [t_{u,a},\, t^{up}_{u,\omega,a},\, t^{dn}_{u,\omega,a}]$. Vector $\bar{\boldsymbol{h}}^{(\boldsymbol{m-1})}$ represents the values of binary variables in $\boldsymbol{h}$ in iteration $m-1$.

$$\sum_{r:\bar{\boldsymbol{h}}^{(\boldsymbol{m-1})}=1} \boldsymbol{h}_r - \sum_{\tilde{r}:\bar{\boldsymbol{h}}^{(\boldsymbol{m-1})}=0} \boldsymbol{h}_{\tilde{r}} \leq |r| - 1 \tag{19}$$

Note that integer cut (19) removes the previous SPNE, but it does not remove any other possible solution from the feasibility region.

4.2. Methodology 2: Representative SPNE approach

Large-scale examples require long computation times to solve MILC model (18), and it might not be practical to find all SPNE. Another way of tackling multiple-SPNE situation is to find a set of representative SPNE where we use a tolerance to control the size of the set of SPNE. To do this, we build a SPNE band, see Fig. 3. We find a lower bound of the best production-cost SPNE[10] and an upper bound of the worst production-cost SPNE. To find the upper bound of the SPNE band, we apply two changes in MILC model (18): (i) Objective function (20a) is added to MILC model (18) and (ii) the integrality constraints on binary variables are relaxed. After applying these changes, the resulting model is a relaxed MILP model and it is set out in (20).

$$\underset{\Gamma \cup \Gamma^{(j)}}{\text{Maximize}} \sum_{\omega} \xi_{\omega} \sum_{u} \hat{c}_u g_{u,\omega} + \sum_{s|\omega} \sigma_{s|\omega} \sum_{u} (\hat{c}^{up} g^{up}_{u,s|\omega} - \hat{c}^{dn} g^{dn}_{u,s|\omega}) \tag{20a}$$

$$\text{Subject to} \tag{20b}$$

$$\text{Constraints } (18b) - (18d) \tag{20c}$$

Note that the integrality constraints on binary variables, $t_{u,a}, t^{up}_{u,\omega,a}, t^{dn}_{u,\omega,a} \in \{0,1\}$, in (18b) and (18c) are relaxed as $t_{u,a}, t^{up}_{u,\omega,a}, t^{dn}_{u,\omega,a} \in [0,1]$. The objective value of maximization model (20) gives us the upper bound of the SPNE band. If maximization model (20) is changed to a minimization model, the new model's objective value gives the lower bound of the SPNE band.

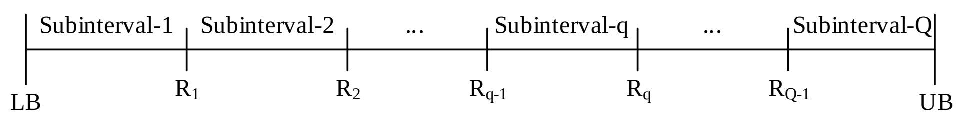

Figure 3: SPNE band, LB: Lower bound of the best-production-cost SPNE, UB: Upper bound of the worst-production-cost SPNE, R_q: Upper bound of subinterval-q.

After finding the upper and the lower bound of the SPNE band, the interval in between is divided into subintervals with a predefined tolerance (ϵ). The number of subintervals is determined by $log_{1+\epsilon} = \frac{UB}{LB}$. The upper bound of each subinterval is calculated as $R_q = (1+\epsilon)R_{q-1}$. A representative SPNE is searched in each subinterval. We model the subintervals by constraint (21). Constraint (21) ensures that the total production cost in the found SPNE in subinterval q is between the lower and upper limits of subinterval q (R_{q-1}, R_q).

$$R_{q-1} \leq \sum_{\omega} \xi_{\omega} \sum_{u} \hat{c}_u g_{u,\omega} + \sum_{s|\omega} \sigma_{s|\omega} \sum_{u} (\hat{c}^{up} g^{up}_{u,s|\omega} - \hat{c}^{dn} g^{dn}_{u,s|\omega}) \leq R_q \tag{21}$$

We include constraint (21) to MILC model (18) and the resulting MILC model is solved in each subinterval. The resulting MILC model related to subinterval q becomes infeasible, if there is no SPNE in subinterval q.

There might not be a SPNE in every subinterval. Thus, to speed up the computation process, we design a pre-feasibility-check method that identifies some of those subintervals

[10] In our paper the best production-cost SPNE is the SPNE with the minimum production cost. The worst production-cost SPNE is the SPNE where the production cost is maximum. Accordingly, all SPNE are located between best- and worst-SPNE.

before solving the model in (18). The pre-feasibility-check method is based on two properties of the duality: (i) The dual of a nonconvex problem is always a convex problem, as shown by Boyd and Vandenberghe (2004), and (ii) if a problem is infeasible, the dual of this problem is unbounded, see Boyd and Vandenberghe (2004). To use these properties, we formulate a nonconvex problem by applying the following two changes: (a) Objective function (22a) is added to MILC model (18) and (b) The bidding decisions of the producers are modeled as continuous variables. The resulting bilinear optimization problem is set out in (22).

$$\underset{\hat{\Gamma}}{\text{Maximize}} \quad \sum_{\omega} \xi_\omega \sum_u \hat{c}_u g_{u,\omega} + \sum_{s|\omega} \sigma_{s|\omega} \sum_u (\hat{c}^{up} g^{up}_{u,s|\omega} - \hat{c}^{dn} g^{dn}_{u,s|\omega}) \tag{22a}$$

$$\text{Subject to} \tag{22b}$$

$$\underline{c}_u \le \hat{c}_u \le \overline{c}_u, \ \forall u \tag{22c}$$

$$\underline{c}^{up}_u \le \hat{c}^{up}_{u,\omega} \le \overline{c}^{up}_u, \ \forall u, \omega \tag{22d}$$

$$\underline{c}^{dn}_u \le \hat{c}^{dn}_{u,\omega} \le \overline{c}^{dn}_u, \ \forall u, \omega \tag{22e}$$

$$\text{Constraints } (10e) - (10i) \tag{22f}$$

$$\text{Constraints } (10e)^{(i),(j)} - (10i)^{(i),(j)}, \ \ \forall i, j \tag{22g}$$

$$\mathbb{E}_{s|\omega}[\phi_{u,s|\omega}] \ge \mathbb{E}_{s|\omega}[\phi^{(i)}_{u,s|\omega}] \ \ \forall u, i \tag{22h}$$

$$\text{Constraints } (16e) - (16l) \tag{22i}$$

$$\text{Constraints } (16e)^{(j)} - (16l)^{(j)}, \ \forall j \tag{22j}$$

$$\mathbb{E}_\omega[\pi_{u,\omega} + \mathbb{E}_{s|\omega}[\phi_{u,s|\omega}]] \ge \mathbb{E}_\omega[\pi^{(j)}_{u,\omega} + \mathbb{E}_{s|\omega}[\phi^{(i),(j)}_{u,s|\omega}]] \ \forall u, i, j \tag{22k}$$

$$R_{q-1} \le \sum_{\omega} \xi_\omega \sum_u \hat{c}_u g_{u,\omega} + \sum_{s|\omega} \sigma_{s|\omega} \sum_u (\hat{c}^{up} g^{up}_{u,s|\omega} - \hat{c}^{dn} g^{dn}_{u,s|\omega}) \le R_q \tag{22l}$$

The set of decision variables in (22) is $\hat{\Gamma} = \{\Gamma \cup \Gamma^{(i)} \backslash \{t_{u,a}, t^{up}_{u,\omega,a}, t^{dn}_{u,\omega,a}, \ t^{(j)}_{u,a}, t^{up,(i),(j)}_{u,\omega,a}, t^{dn,(i),(j)}_{u,\omega,a}\}$. Here parameters $\overline{c}_u$, $\overline{c}^{up}_u$, $\overline{c}^{dn}_u$ and $\underline{c}_u$, $\underline{c}^{up}_u$, $\underline{c}^{dn}_u$ are the upper and lower limits of $\hat{c}_u$, $\hat{c}^{up}_{u,\omega}$, $\overline{c}^{dn}_{u,\omega}$. The BLP model in (22) is a relaxation of MILC model (18) therefore if BLP model (22) in subinterval q is infeasible, MILC model (18) is also infeasible in subinterval q of the SPNE band. This means that there is no SPNE in subinterval q. Here we use the property (i) of duality described above and take the dual of BLP model (22). The dual program is a LP model and it is easier to solve compared to BLP model (22). We solve the dual problem in each subinterval. We may face two cases: (i) if the dual problem has a finite solution, there might be a SPNE in this subinterval or (ii) if the dual problem is unbounded, there is no SPNE in this subinterval. Note that due to the nonconvexity of the BLP problem, in some subintervals we may have a finite dual solution, even though there is no SPNE. However if the dual problem is unbounded in a subinterval, then it is guaranteed that there is no SPNE in this subinterval.

Using this method, we identify the subintervals which have no SPNE, omit those subintervals, and then we search for the SPNE in the remaining subintervals. The pre-feasibility-check method improves the computational tractability for finding the set of representative SPNE.

5. Illustrative Example

This section demonstrates the producers' bidding behaviors under different zonal pricing approaches on the 6-node example system which was used by Chao and Peck (1998). We consider one delivery hour. Fig. 4 shows the single line diagram of the 6-node example system. We introduce two zones. Zone 1 aggregates nodes 1, 2 and 3. Zone 2 aggregates nodes 4, 5 and 6. The 6-node example system has 3 competing producers u_1, u_2 and u_3 which are located at nodes 1, 2 and 4, respectively. The data related to the producers is presented in Table 5. The variation in marginal cost for up- and down-regulation of a unit corresponds to a switching cost. The switching cost is due to the fact that in the real-time market, a unit has to change its production in a relatively short notice, see Morales et al. (2014). To have a congested network and to observe an inc-dec game, the transmission capacity of the lines between nodes 1-2, 2-5 and 1-6 are set to 35 MW, 70 MW and 65 MW, respectively. The transmission capacity of the other lines is set to 100 MW. For the day-ahead market, the flow limit between zones 1 and 2 is set to 110 MW in order to have different day-ahead prices in different zones. The consumers located at nodes 2, 5 and 6 have fixed demand of 120 MW, 100 MW and 60 MW, respectively.

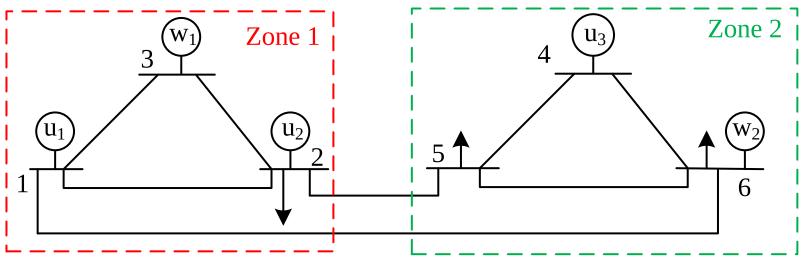

Figure 4: Single line diagram of the 6-node example system, u_1,u_2, u_3: Conventional producers, W_1, W_2: Wind farms.

Two wind farms are connected to nodes 3 and 6. Two wind-generation scenarios are considered: W_{n,ω_1} =30 MW and W_{n,ω_2} =37.5 MW. In real-time, the deviation from the net demand ($\Delta W_{n,s|\omega}$) is modeled with 2 scenarios. Scenario s_1 represents the positive imbalance scenario ($\Delta W_{n,s_1|\omega} = 0.2 W_{n,\omega}$), scenario s_2 represents the negative imbalance scenario ($\Delta W_{n,s_2|\omega} = -0.2 W_{n,\omega}$). The probabilities for the scenarios are equal. We assume that each producer has 3 bidding actions for day-ahead price bids with 0%, 10% mark-up and 10% mark-down. In real-time, the permissible up-regulation and down-regulation bids have 0%, 10%, 20% mark-up and 0%, 10%, 20% mark-down, respectively.

Table 5: Unit data for the 6-node system

Unit	C ($/MWh)	C^{up} ($/MWh)	C^{dn} ($/MWh)	G_u (MW)
u_1	11.5	23	7.5	150
u_2	10.5	21	6.5	250
u_3	13	25	8.5	150

Table 6 summarizes the five approaches that we simulate. In addition to Approaches 1 (UK) and 2 (Optimal zonal), we also simulate a benchmark approach (BA) and two approaches with truthful bidding: WAL and WALZ. BA has nodal pricing both in the day-ahead and real-time market, and considers strategic bidders. WAL (Walrasian) considers the same nodal system, but with naive truthful bidders. WALZ also consider truthful bidders, but for the market design A2.

In SPNE, all producers submit their equilibrium bids ($\hat{c}_u$) to the day-ahead market. A short

Table 6: Simulated approaches

Approach	Explanation
Approach 1 (A1)	Zonal day-ahead and pay-as-bid in real-time
Approach 2 (A2)	Zonal day-ahead and optimal zonal in real-time
Benchmark approach (BA)	Nodal day-ahead and nodal in real-time
Walrasian (WAL)	Naive competitive bidding in BA
Walrasian zonal (WALZ)	Naive competitive bidding in A2

time before the delivery hour, units u_1, u_2 and u_3 consider the day-ahead dispatch (including the wind-power output) and submit their regulation bids to the real-time market. We use methodology 1 to tackle multiple SPNE in this example system. Some SPNE are essentially the same, i.e. the payment, cost and output is the same for each producer. For example, the bid price of a rejected equilibrium bid does not matter much as long as all accepted equilibrium bids are the same. In Table 7, we report each distinct SPNE for each market design. We found one distinct SPNE for Approach 1 and the benchmark approach. In Approach 2, we found two SPNE (A2-1 and A2-2) with different dispatches, production costs and payments. Multiplicity of equilibria was not a major issue in this study. We believe that the shocks in our model has reduced this problem. Multiplicity of equilibria was more of a problem in a related study, Sarfati et al. (2019), where we did not consider shocks.

Table 7: The SPNE for each approach, A1: Approach 1, A2: Approach 2, BA: Benchmark, approach, A2-1: First SPNE in Approach 2

	u_1			u_2			u_3		
	$\hat{c}_u$	$(\hat{c}^{up}_{u,\omega},\hat{c}^{dn}_{u,\omega})$		$\hat{c}_u$	$(\hat{c}^{up}_{u,\omega},\hat{c}^{dn}_{u,\omega})$		$\hat{c}_u$	$(\hat{c}^{up}_{u,\omega},\hat{c}^{dn}_{u,\omega})$	
		ω_1	ω_2		ω_1	ω_2		ω_1	ω_2
A1	10.35	(23,6)	(23,6)	11.55	(25.2,5.2)	(25.2,5.2)	14.3	(30,8.5)	(30,8.5)
A2-1	12.65	(27.6,6)	(27.6,6)	11.55	(25.2,5.2)	(25.2,5.2)	14.3	(30,6.8)	(30,6.8)
A2-2	11.5	(23,6)	(23,6)	10.5	(25.2,5.2)	(25.2,5.2)	14.3	(30,6.8)	(30,6.8)
BA	11.5	(27.6,6)	(27.6,6)	11.55	(25.2,5.2)	(25.2,5.2)	14.3	(30,6.8)	(30,6.8)

Table 7 shows that in Approach 1, producer u_1 chooses a day-ahead bid which is lower than its marginal cost, which is consistent with an inc-dec strategy, see Harvey and Hogan (2000a). Table 8 presents further results that are consistent with the inc-dec game. It shows that the day-ahead dispatches in Approach 1 overload the intra-zonal line, line 1-2, by 32.1 MW in scenario ω_1 and by 34.6 MW in scenario ω_2. Here node 1 is the export-constrained node and node 2 is the import-constrained node. To relieve this overloading, the system operator accepts u_1's down-regulation bid and u_2's up-regulation bid in every scenario. Accordingly, producer u_1 buys back power and producer u_2 sells power in the real-time market. The counter-traded volume in each scenario is reported in Table 8.

Table 9 shows that producer u_1 increases its total expected profit by at least nine times in Approach 1 as compared to the benchmark approach (nodal pricing) due to the inc-dec game.

Table 10 shows that the inc-dec game, in Approach 1, increases the total profit of the producers by 47.7% as compared to the benchmark approach. Approach 2 is designed to reduce the inc-dec game by setting the price in the day-ahead and real-time markets in a similar way, which reduces arbitrage opportunities. Indeed, we observe that in Approach 2,

Table 8: Overloaded volume in line 1-2 and the counter-traded volume in the real-time market for Approach 1

Scenario ω	Overloaded volume in Line 1-2 (MW)	Scenario $s\|\omega$	Counter-traded volume (MWh)
ω_1	32.1	$s_1\|\omega_1$	49.4
		$s_2\|\omega_1$	48.6
ω_2	34.6	$s_1\|\omega_2$	52.3
		$s_2\|\omega_2$	51.2

Table 9: The profit of each producer for each real-time pricing approach, A1: Approach 1, A2: Approach 2, BA: Benchmark approach, A2-1: First SPNE in Approach 2

	Expected profit (\$/h) (in the day-ahead market)			Expected profit (\$/h) (in the real-time market)			Expected profit (\$/h) (Total)		
	u_1	u_2	u_3	u_1	u_2	u_3	u_1	u_2	u_3
A1	7.5	48.6	21.1	85.7	240	0	93.2	288.5	21.1
A2-1	0	206.1	21.1	0	29.2	15.4	0	235.3	36.5
A2-2	0	0	21.1	0	0.8	15.4	0	0.8	36.5
BA	0	234.2	0	10.1	28.1	0.4	10.1	262.3	0.4

the day-ahead dispatches do not overload any line in the network, when the producers bid their strategic day-ahead bids (A2) or their marginal costs (WALZ) to the day-ahead market. This causes a significant decrease in the profit of u_1 in Approach 2 compared to its profit in Approach 1. Similarly, we see in Table 10 that total profit for Approach 2 is similar to the benchmark approach for SPNE in A2-1. For SPNE in A2-2, Approach 2 could even have significantly lower total profit compared to nodal pricing.

Table 10: The production costs, the total profit of all producers and the switching cost for each real-time pricing approach, DAM: Day-ahead market, RTM: Real-time market, WAL: Naive competitive bidding in BA, WALZ: Naive competitive bidding in A2

	Production cost in the DAM (\$/h)	Energy-only production cost in the RTM (\$/h)	Switching cost in the RTM (\$/h)	Total production cost (\$/h)	Total profit of all producers (\$/h)
WAL	2246.9	107.1	104	2354	1.3
WALZ	2271.9	85.6	100.9	2357.5	6.3
A1	2421.9	771.3	828.4	3193.2	402.9
A2-1	2271.9	85.6	100.9	2357.5	271.8
A2-2	2271.9	99.1	107.7	2371	37.4
BA	2332.2	91.4	98	2423.6	272.7

Strategic bidding can also lead to inefficiences, e.g. higher (true) production costs. Table 10 presents the production cost in the day-ahead and real-time markets for each approach. The production cost in the day-ahead market is the production cost corresponding to the day-ahead dispatch. The real-time production cost is an extra cost due to real-time deviations from the day-ahead dispatch. We divide the real-time cost into two parts: 1) an energy-only cost due to the extra energy that is produced in real-time and 2) a ramping or switching cost (SWC)[11].

The benchmark approach with nodal pricing has roughly the same total production cost as Approach 2, both for A2-1 and A2-1. In its turn, Approach 2 has a much lower total production cost than Approach 1. One reason for this is that the switching cost is about 8 times higher in Approach 1. The inc-dec game is very pronounced for Approach 1. This drastically increases the traded real-time volume and therefore also the switching costs.

Inefficiences are less problematic for A2 and BA. Strategic bidding in the benchmark approach increases the toal production cost by 3% compared to the case WAL. Depending on equilibrium selection, strategic bidding in Approach 2 increases the total production cost by 0-0.6% compared to the case WALZ. The latter inefficiences seem small, given that mark-ups are significant. One reason for the small inefficiences is that in our model, with inelastic demand, mark-ups only lead to inefficiences when they change the merit order. Another reason is that we assume the Colombian bidding format with one bid price per plant. It is known from the previous literature, Holmberg and Wolak (2018) and Anderson and Holmberg (2018), that markets can be fully efficient under those two circumstances, even if producers exercise market power.

In this example system, each producer has 3x3=9 (3 up-regulation, 3 down-regulation) strategies for each scenario ω. We consider 2 wind-production scenarios in the day-ahead market, so each producer has 9x9=81 possible strategies when deciding on the real-time bid. Each producer also has three possible strategies for its day-ahead bid. Thus, in the two-stage game, each producer has 81x3=243 possible strategies. Since we have 3 producers in the example system, the total number of bid combinations is 14,348,907. If we iterate over each of these combinations and each solution takes hypothetically 1 second, the computation of the SPNE will take approximately 166 days. However our MILC model can compute the SPNE in moderate time.

6. IEEE 24-node example system

An original version of the IEEE 24-node example system is presented by Grigg et al. (1999). In this section, we modify this example somewhat and use it to compare the zonal pricing designs and demonstrate our proposed model on a larger system. We consider three zones. Zone 1 aggregates nodes 15-23. Zone 2 aggregates nodes 11-14 and 24. Zone 3 aggregates nodes 1-10. The data related to the producers is presented in Table 11.

The transmission capacity of the lines between nodes 1-2, 3-24, 14-16 and 21-22 are set to 200 MW, 220 MW, 220 MW and 425 MW, respectively. For the day-ahead market, the system operator sets the flow limits between zones 1 and 2 to 400 MW and between zones 2 and 3 to 820 MW.

Five wind farms are connected to nodes 8, 11, 12, 16 and 23. One wind-generation scenario (W_{n,ω_1}=171 MW) is considered in the day-ahead market. The deviation from the net demand ($\Delta W_{n,s|\omega}$) is modeled with 11 scenarios. The coefficient (Υ_s) for each scenario is shown in Table 12. The deviation from the net demand in each scenario is calculated by $\Delta W_{n,s|\omega_1} = \Upsilon_s W_{n,\omega_1}$. Scenarios s_1, s_2, s_3, s_4, and s_5 represent the positive-imbalance scenarios, scenario s_6 represents

[11] We define switching cost as the dispatch in the real-time market times the difference between the marginal regulation costs and the marginal cost. Mathematically, we can express it as $SWC = \sum_{\omega,s} \sigma_{s|\omega}(\sum_u((C_u^{up} - C_u)g_{u,s|\omega}^{up} + (C_u - C_u^{dn})g_{u,s|\omega}^{dn}))$.

Table 11: Unit data for IEEE 24-node system

Unit	node	C (\$/MWh)	C^{up} (\$/MWh)	C^{dn} (\$/MWh)	G_u (MW)
u_1	1	19	27.1	11	500
u_2	2	15.5	23.5	11.5	400
u_3	13	14.5	22.5	9.5	450
u_4	21	13	20.5	7	1100
u_5	22	13.5	21.5	8.5	1100

Table 12: The net demand deviation scenarios, Υ_s: Coefficient, $\Delta W_{n,s|\omega_1} = \Upsilon_s W_{n,\omega_1}$

	s_1	s_2	s_3	s_4	s_5	s_6	s_7	s_8	s_9	s_{10}	s_{11}
Υ_s	0.18	0.15	0.12	0.09	0.06	0	-0.06	-0.09	-0.12	-0.15	-0.18

the no-imbalance scenario and scenarios s_7, s_8, s_9, s_{10}, and s_{11} represent the negative-imbalance scenarios. We assume that each producer has 3 bidding actions for day-ahead price bids: 0%, 10% mark-up and 10% mark-down. For up- and down-regulation bids in the real-time market, we allow for 0%, 10%, 20% mark-up and 0%, 10%, 20% mark-down, respectively.

Table 13: The SPNE search in the subintervals, A1: Approach 1, A2: Approach 2, BA: Benchmark approach, SI: Subinterval, LB: Lower bound, UB: Upper bound, No SPNE: No SPNE is found in this subinterval, SPNE: SPNE is found in this subinterval

	LB of SI_q	UB of SI_q	A1	A2	BA
SI_1	25389.7	27928.7	No SPNE*	No SPNE*	No SPNE*
SI_2	27928.7	30721.6	No SPNE	No SPNE	No SPNE
SI_3	30721.6	33793.7	No SPNE	**SPNE**	**SPNE**
SI_4	33793.7	37173.1	**SPNE**	No SPNE	No SPNE
SI_5	37173.1	40890.4	No SPNE	No SPNE	No SPNE*
SI_6	40890.4	44979.5	No SPNE*	No SPNE*	No SPNE*
SI_7-SI_{11}	44979.5	71617	No SPNE*	No SPNE*	No SPNE*

We apply methodology 2 to tackle multiple SPNE. The lower and upper bound of the SPNE band is calculated as 25389.7 \$/h and 71617 \$/h for all four approaches. The tolerance is set to 10% and the SPNE band is split into 11 subintervals. Then we run the pre-feasibility-check method in all subintervals. Table 13 shows that, according to the pre-feasibility check, there are no SPNE in the subintervals marked by *. These subintervals are omitted and no SPNE is searched. In Approach 1 and Approach 2, we search a representative SPNE in subintervals between SI_2-SI_5. For Approach 1, we find a representative SPNE in SI_4, but not in SI_2, SI_3, SI_5 and SI_6. For Approach 2 and the benchmark approach, a representative SPNE in SI_3 is found.

Table 14 shows that in Approach 1, u_5 chooses a day-ahead bid which is lower than its marginal cost and becomes the cheapest producer in the market. We observe in Table 15 that the day-ahead dispatches in Approach 1 overload the intra-zonal line between nodes 21 and

*The pre-feasibility check reports that there is no SPNE in this subinterval.

Table 14: The representative SPNE in each approach, A1: Approach 1, A2: Approach 2, BA: Benchmark approach, $\hat{c}_u$: Day-ahead price bid ($/MWh), $(\hat{c}^{up}_{u,\omega_1}, \hat{c}^{dn}_{u,\omega_1})$: Up- and down-regulation price bid ($/MWh, $/MWh)

		u_1	u_2	u_3	u_4	u_5
A1	$\hat{c}_u$	20.9	17.05	15.95	14.3	12.15
	$(\hat{c}^{up}_{u,\omega_1}, \hat{c}^{dn}_{u,\omega_1})$	(27.1,11)	(25.85,11.5)	(27,9.5)	(24.6,7)	(21.5,6.8)
A2	$\hat{c}_u$	20.9	17.05	15.95	14.3	14.85
	$(\hat{c}^{up}_{u,\omega_1}, \hat{c}^{dn}_{u,\omega_1})$	(32.52,9.9)	(23.5,9.2)	(22.5,7.6)	(22.55,5.6)	(25.8,6.8)
BA	$\hat{c}_u$	20.9	17.05	15.95	14.3	14.85
	$(\hat{c}^{up}_{u,\omega_1}, \hat{c}^{dn}_{u,\omega_1})$	(32.52,9.9)	(28.2,9.2)	(27,8.55)	(24.6,6.3)	(25.8,6.8)

22 by 233.5 MW. To relieve this overloading, the volumes reported in Table 15 are counter-traded in the real-time market. In Approach 1, producers u_4 and u_5 provide the necessary up-regulation (u_4) and down-regulation (u_5) for counter-trading. In contrast, we observe that no transmission line is overloaded when the producers bid their strategic day-ahead bids (A2) or their marginal costs (WALZ) to the day-ahead market in Approach 2.

Table 15: The counter-traded volume in the real-time market for Approach 1

	s_1	s_2	s_3	s_4	s_5	s_6	s_7	s_8	s_9	s_{10}	s_{11}
Counter-traded volume (MWh)	127.6	166.6	205.5	244.4	283.4	361.3	353.6	349.8	346.8	342.2	338.4

Table 16: The profit of each producer in each real-time pricing approaches; π_u ($/h): Profit in the day-ahead market, Φ_u ($/h): Expected profit in the real-time market, Δ_u ($/h): Total profit in both markets

	Approach 1			Approach 2			Benchmark approach		
	π_u	Φ_u	Δ_u	π_u	Φ_u	Δ_u	π_u	Φ_u	Δ_u
u_1	43.7	0	43.7	43.7	18.5	62.2	0	15	15
u_2	2160	0	2160	2160	83.2	2243.2	470.1	322.8	792.9
u_3	2880	0	2880	2880	0	2880	1192.9	0	1192.9
u_4	22.1	1481.2	1503.3	2035	0	2035	2054.6	0	2054.6
u_5	880	614.2	1494.2	23	199.6	222.6	184.5	58.1	242.6

The inc-dec game is mainly profitable for export-constrained producers. Table 16 shows that u_5 (located at the export-constrained node) increases its total profit by at least five times in Approach 1, compared to the benchmark approach. But the inc-dec game reduces the total profit of u_4 (located at the import-constrained node) by 24.6% in Approach 1 compared to the benchmark approach. The total profit of producers is lower in Approach 2 in comparison to Approach 1. The benchmark approach has significantly lower profits compared to both A1 and A2.

Table 17 illustrates that Approach 2 has the lowest total production cost and Approach 1 has the highest total production cost among the zonal market designs. Employing Approach 2 in the real-time market reduces the total production cost by 13.5% as compared to Approach 1. Again this can be partly explained by that the switching cost is much higher in Approach 1, because of the inc-dec game. We observe that the total production cost in Approach 2 and in WALZ are roughly the same.

Table 17: The production costs, the total profit of all producers and the switching cost for real-time pricing approach, DAM: Day-ahead market, RTM: Real-time market, WAL: Naive competitive bidding in BA, WALZ: Naive competitive bidding in A2

	Production cost in the DAM ($/h)	Energy-only production cost in the RTM ($/h)	Switching cost in the RTM ($/h)	Total production cost ($/h)	Total profit of all producers ($/h)
WAL	27371.6	579.3	569.6	27950.9	1123.4
WALZ	27691.6	467.6	559.7	28159.2	3975.0
A1	28233	4335.2	4515.8	32568.2	8081.2
A2	27691.5	472.8	601.5	28164.3	7443.0
BA	27371.6	579.3	569.6	27950.9	4298.1

7. Conclusion

This paper applies a two-stage game to study imperfect competition and arbitrage strategies of producers in zonally-priced electricity markets with a day-ahead and a real-time market. The two-stage game is mathematically formulated as a two-stage stochastic EPEC and it is recast into a two-stage stochastic MILC model which can be solved by the commercial solvers. The multiple-SPNE issue is tackled by two methodologies. In the first methodology, we find all SPNE using an iterative procedure. This methodology is relevant in small networks where the computation of a SPNE is possible in short time. In methodology 2, we build a SPNE band which consists of all SPNE. Then the SPNE band is divided into several subintervals and a representative SPNE is found in each subinterval. This methodology is relevant for larger networks. The proposed MILC model and the methodologies to tackle the multiple-SPNE issue are applied to the 6-node and IEEE 24-node example systems.

Our numerical results illustrate that the inc-dec game can lead to large production inefficiencies and large profits for producers in zonal electricity markets in comparison to nodal pricing. However, our results also illustrate how the inc-dec game can be mitigated, at least in our examples.

We believe that the inc-dec game can be mitigated by making the real-time market design more similar to the day-ahead zonal design, which should reduce arbitrage opportunities. This can for example be done by minimizing real-time price differences within each zone. This may not always be feasible in practice, but in the cases that we simulate, we are able to reduce price differences all the way down to zero. In the networks that we simulate, we do this by simply constraining real-time price differences to be zero within each zone. This corresponds to optimal zonal pricing. All else equal (including identical bids), such a constraint leads to an inefficient dispatch. But if the inc-dec problem is severe, then overall inefficiency can improve if bidding behaviour changes and becomes less problematic.

We simulate both the 6-node and 24-node networks for a zonal day-ahead market and pay-as-bid in real time. The inc-dec game is severe in both networks. In both cases the inc-dec game is mitigated, and overall efficiency significantly improved, after introducing optimal-zonal pricing in the real-time market.

Acknowledgments

Mahir Sarfati was sponsored by the Swedish Centre for Smart Grids and Energy Storage (SweGRIDS). Pär Holmberg and Mahir Sarfati have been financially supported by the Jan Wallanders och Tom Hedelius stiftelse and the Swedish Energy Agency.

References

Ahlqvist, V., Holmberg, P., Tangerås, T., 2018. Central- versus Self-Dispatch in Electricity Markets. IFN Working Papers 1257. Research Institute Of Industrial Economics (IFN). URL: `https://www.ifn.se/publikationer/working_papers/2018/1257`.

Alaywan, Z., Wu, T., Papalexopoulos, A.D., 2004. Transitioning the california market from a zonal to a nodal framework: an operational perspective, in: IEEE PES Power Systems Conference and Exposition, 2004., pp. 862–7.

Anderson, E., Holmberg, P., 2018. Price instability in multi-unit auctions. Journal of Economic Theory 175, 318 –41.

Bakirtzis, A.G., Ziogos, N.P., Tellidou, A.C., Bakirtzis, G.A., 2007. Electricity producer offering strategies in day-ahead energy market with step-wise offers. IEEE Transactions on Power Systems 22, 1804–18. doi:10.1109/TPWRS.2007.907536.

Barroso, L.A., Carneiro, R.D., Granville, S., Pereira, M.V., Fampa, M.H.C., 2006. Nash equilibrium in strategic bidding: a binary expansion approach. IEEE Transactions on Power Systems 21, 629–38. doi:10.1109/TPWRS.2006.873127.

van den Bergh, K., Boury, J., Delarue, E., 2016. The flow-based market coupling in central western europe: Concepts and definitions. The Electricity Journal 29, 24 –9.

Bjørndal, E., Bjørndal, M., Gribkovskaia, V., 2012. Congestion management in the Nordic power market: nodal pricing versus zonal pricing. Technical Report 15. SNF. NHH. URL: `https://www.snf.no/Files/Filer/Publications/R15_12.pdf`.

Bjørndal, E., Bjørndal, M., Rud, L., 2013. Congestion management by dispatch or re-dispatch: Flexibility costs and market power effects, in: 2013 10th International Conference on the European Energy Market (EEM), pp. 1–8. doi:10.1109/EEM.2013.6607346.

Bjørndal, M., Jørnsten, K., 2001. Zonal pricing in a deregulated electricity market. The Energy Journal 22, 51–73. URL: `http://www.jstor.org/stable/41322907`.

Bjørndal, M., Jörnsten, K., 2007. Benefits from coordinating congestion management—the nordic power market. Energy Policy 35, 1978 –91.

Blázquez de Paz, M., 2018. Electricity auctions in the presence of transmission constraints and transmission costs. Energy Economics 74, 605 –27.

Boyd, S., Vandenberghe, L., 2004. Convex Optimization. Cambridge University Press, New York, NY, USA.

Brandts, J., Reynolds, S.S., Schram, A., 2014. Pivotal suppliers and market power in experimental supply function competition. The Economic Journal 124, 887–916.

Chao, H.P., Peck, S., 1998. Reliability management in competitive electricity markets. Journal of Regulatory Economics 14, 189–200.

Dijk, J., Willems, B., 2011. The effect of counter-trading on competition in electricity markets. Energy Policy 39, 1764–73.

von der Fehr, N.H.M., Harbord, D., 1993. Spot market competition in the uk electricity industry. The Economic Journal 103, 531–46.

Gabriel, S., Conejo, A., Fuller, J., Hobbs, B., Ruiz, C., 2012. Complementarity Modeling in Energy Markets. International Series in Operations Research & Management Science, Springer New York.

Green, R., 2007. Nodal pricing of electricity: how much does it cost to get it wrong? Journal of Regulatory Economics 31, 125–49.

Grigg, C., Wong, P., Albrecht, P., Allan, R., Bhavaraju, M., Billinton, R., Chen, Q., Fong, C., Haddad, S., Kuruganty, S., Li, W., Mukerji, R., Patton, D., Rau, N., Reppen, D., Schneider, A., Shahidehpour, M., Singh, C., 1999. The ieee reliability test system-1996. a report prepared by the reliability test system task force of the application of probability methods subcommittee. IEEE Transactions on Power Systems 14, 1010–20.

Gupte, A., Ahmed, S., Cheon, M.S., Dey, S., 2013. Solving mixed integer bilinear problems using milp formulations. SIAM Journal on Optimization 23, 721–44. doi:10.1137/110836183.

Harvey, S.M., Hogan, W.W., 2000a. Nodal and zonal congestion management and the exercise of market power. Harvard University URL: http://www.lmpmarketdesign.com/papers/zonal_jan10.pdf.

Harvey, S.M., Hogan, W.W., 2000b. Nodal and zonal congestion management and the exercise of market power: Further comments. Harvard University URL: https://sites.hks.harvard.edu/fs/whogan/zonal_Feb11.pdf.

Hesamzadeh, M.R., Biggar, D.R., 2012. Computation of extremal-nash equilibria in a wholesale power market using a single-stage MILP. Power Systems, IEEE Transactions on 27, 1706–7. doi:10.1109/TPWRS.2012.2187120.

Hesamzadeh, M.R., Biggar, D.R., 2013. Merger analysis in wholesale power markets using the equilibria-band methodology. IEEE Transactions on Power Systems 28, 819–27.

Hesamzadeh, M.R., Holmberg, P., Sarfati, M., 2018. Simulation and Evaluation of Zonal Electricity Market Designs. IFN Working Papers 1211. Research Institute of Industrial Economics (IFN). URL: https://www.ifn.se/publikationer/working_papers/2018/1211.

Hirth, L., Schlecht, I., Maurer, C., Tersteegen, B., 2019. Cost- or market-based? Future redispatch procurement in Germany. Technical Report. Neon Neue Energieökonomik GmbH. URL: https://www.bmwi.de/Redaktion/EN/Publikationen/Studien/future-redispatch-procurement-in-germany.pdf?__blob=publicationFile&v=3.

Holmberg, P., Lazarczyk, E., 2015. Comparison of congestion management techniques: Nodal, zonal and discriminatory pricing. Energy Journal 36, 145 –66.

Holmberg, P., Newbery, D., Ralph, D., 2013. Supply function equilibria: Step functions and continuous representations. Journal of Economic Theory 148, 1509 –51.

Holmberg, P., Willems, B., 2015. Relaxing competition through speculation: Committing to a negative supply slope. Journal of Economic Theory 159, 236 –66.

Holmberg, P., Wolak, F.A., 2018. Comparing auction designs where suppliers have uncertain costs and uncertain pivotal status. RAND Journal of Economics .

Hortaçsu, A., Puller, S.L., 2008. Understanding strategic bidding in multi-unit auctions: a case study of the texas electricity spot market. The RAND Journal of Economics 39, 86–114.

Hu, X., Ralph, D., 2007. Using epecs to model bilevel games in restructured electricity markets with locational prices. Operations research 55, 809–27.

Moiseeva, E., Hesamzadeh, M.R., 2018. Bayesian and robust nash equilibria in hydrodominated systems under uncertainty. IEEE Transactions on Sustainable Energy 9, 818–30. doi:10.1109/TSTE.2017.2762086.

Moiseeva, E., Hesamzadeh, M.R., 2018. Strategic bidding of a hydropower producer under uncertainty: Modified benders approach. IEEE Transactions on Power Systems 33, 861–73.

Morales, J.M., Conejo, A.J., Madsen, H., Pinson, P., Zugno, M., 2014. Integrating renewables in electricity markets: operational problems. Springer Science & Business Media.

Neuhoff, K., Hobbs, B., Newbery, D.M., 2011. Congestion Management in European Power Networks: Criteria to Assess the Available Options. Discussion Papers of DIW Berlin 1161. DIW Berlin, German Institute for Economic Research.

Pereira, M.V., Granville, S., Fampa, M.H.C., Dix, R., Barroso, L.A., 2005. Strategic bidding under uncertainty: a binary expansion approach. IEEE Transactions on Power Systems 20, 180–8. doi:10.1109/TPWRS.2004.840397.

Ruderer, D., Zöttl, G., 2012. The impact of transmission pricing in network industries. Cambridge Working Papers in Economics 1230. Faculty of Economics, University of Cambridge.

Ruiz, C., Conejo, A.J., Gabriel, S.A., 2012. Pricing non-convexities in an electricity pool. IEEE Transactions on Power Systems 27, 1334–42.

Sarfati, M., Hesamzadeh, M.R., Holmberg, P., 2018a. Increase-Decrease Game under Imperfect Competition in Two-stage Zonal Power Markets – Part I: Concept Analysis. IFN Working Papers 1253. Research Institute Of Industrial Economics (IFN). URL: https://www.ifn.se/publikationer/working_papers/2018/1253.

Sarfati, M., Hesamzadeh, M.R., Holmberg, P., 2018b. Increase-Decrease Game under Imperfect Competition in Two-stage Zonal Power Markets – Part II: Solution Algorithm. IFN Working Papers 1254. Research Institute Of Industrial Economics (IFN). URL: https://www.ifn.se/publikationer/working_papers/2018/1254.

Sarfati, M., Hesamzadeh, M.R., Holmberg, P., 2019. Production efficiency of nodal and zonal pricing in imperfectly competitive electricity markets. Energy Strategy Reviews 24, 193–206.

Schwenen, S., 2015. Strategic bidding in multi-unit auctions with capacity constrained bidders: the new york capacity market. The RAND Journal of Economics 46, 730–50.

Sioshansi, R., Oren, S., 2007. How good are supply function equilibrium models: an empirical analysis of the ercot balancing market. Journal of Regulatory Economics 31, 1–35.

Stoft, S., 1999. Financial transmission rights meet cournot: How tccs curb market power. The Energy Journal 20, 1–23.

Willems, B., 2002. Modeling cournot competition in an electricity market with transmission constraints. The Energy Journal 23, 95–125.

Wolak, F.A., 2007. Quantifying the supply-side benefits from forward contracting in wholesale electricity markets. Journal of Applied Econometrics 22, 1179–209.

Wolak, F.A., 2009. Report on Market Performance and Market Monitoring in the Colombian Electricity Supply Industry. Technical Report. Superintendencia de Servicios Públicos (SSPD). URL: https://web.stanford.edu/group/fwolak/cgi-bin/sites/default/files/files/sspd_report_wolak_july_30.pdf.

Zhang, D., Kim, S., 2010. A two stage stochastic equilibrium model for electricity markets with forward contracts, in: Proc. 2010 11th International Conference on Probabilistic Methods Applied to Power Systems (PMAPS), pp. 194–9.

Zhang, D., Xu, H., 2013. Two-stage stochastic equilibrium problems with equilibrium constraints: modeling and numerical schemes. Optimization 62, 1627–50.

Zhang, D., Xu, H., Wu, Y., 2010. A two stage stochastic equilibrium model for electricity markets with two way contracts. Mathematical Methods of Operations Research 71, 1–45.

Appendix A. The details of replacement of complementary slackness conditions by strong duality conditions

Let's consider the bidding problem of a producer in the real-time pricing approach in Approach 1. It is modeled in bilevel optimization problem (A.1).

$$\underset{\hat{c}^{up}_{u,\omega},\hat{c}^{dn}_{u,\omega},t^{up}_{u,\omega,a},t^{dn}_{u,\omega,a}}{\text{Maximize}} \quad \mathbb{E}_{s|\omega}[\phi_{u,s|\omega}] = \sum_{s|\omega}(\hat{c}^{up}_{u,\omega} - C^{up}_{u})g^{up}_{u,s|\omega} + (C^{dn}_{u} - \hat{c}^{dn}_{u,\omega})g^{dn}_{u,s|\omega} \tag{A.1a}$$

Subject to:

$$\hat{c}^{up}_{u,\omega} = \sum_{a} B^{up}_{a} t^{up}_{u,\omega,a} C^{up}_{u}, \quad \hat{c}^{dn}_{u,\omega} = \sum_{a} B^{dn}_{a} t^{dn}_{u,\omega,a} C^{dn}_{u} \tag{A.1b}$$

$$t^{up}_{u,\omega,a}, t^{dn}_{u,\omega,a} \in \{0,1\} \tag{A.1c}$$

$$\sum_{a} t^{up}_{u,\omega,a} = 1, \quad \sum_{a} t^{dn}_{u,\omega,a} = 1 \tag{A.1d}$$

$$\text{where}\{g^{up}_{u,s|\omega}, g^{dn}_{u,s|\omega}, v_{n,s|\omega}\} \in \left\{ \underset{g^{up}_{u,s|\omega},g^{dn}_{u,s|\omega},v_{n,s|\omega}}{\text{argMinimize}} \quad \sum_{s|\omega,u} \sigma_{s|\omega}(\hat{c}^{up}_{u,\omega} g^{up}_{u,s|\omega} - \hat{c}^{dn}_{u,\omega} g^{dn}_{u,s|\omega}) \right. \tag{A.1e}$$

Subject to:

$$\sum_{u}(g_{u,\omega} + g^{up}_{u,s|\omega} - g^{dn}_{u,s|\omega}) = \sum_{n}(v_{n,s|\omega} + D_{n,\omega} - \Delta W_{n,s|\omega}) : (\alpha_{s|\omega}) \ \forall s|\omega \tag{A.1f}$$

$$F_k - \sum_{n} H_{k,n}(\sum_{u} \Psi_{u,n}(g_{u,\omega} + g^{up}_{u,s|\omega} - g^{dn}_{u,s|\omega}) - v_{n,s|\omega} - D_{n,\omega} + \Delta W_{n,s|\omega}) \geq 0 :$$
$$(\mu_{k,s|\omega}), \ \forall k, s|\omega \tag{A.1g}$$

$$0 \leq g^{up}_{u,s|\omega} \leq (G_u - g_{u,\omega}) : (\kappa_{u,s|\omega}, \beta_{u,s|\omega}) \ \forall u, s|\omega \tag{A.1h}$$

$$0 \leq g^{dn}_{u,s|\omega} \leq g_{u,\omega} : (\psi_{u,s|\omega}, \varphi_{u,s|\omega}) \ \forall u, s|\omega \tag{A.1i}$$

$$\left. 0 \leq v_{n,s|\omega} \leq \bar{W}_{n,\omega} + \Delta W_{n,s|\omega} : (\theta_{n,s|\omega}, \chi_{n,s|\omega}) \right\} \tag{A.1j}$$

The inner optimization problem is in (A.1e)-(A.1j). The complementary slackness conditions of (A.1e)-(A.1j) is set out in (A.2).

$$\mu_{k,s|\omega}\big(F_k - \sum_{n} H_{k,n}(\sum_{u} \Psi_{u,n}(g_{u,\omega} + g^{up}_{u,s|\omega} - g^{dn}_{u,s|\omega}) - v_{n,s|\omega} -$$
$$D_{n,\omega} + \Delta W_{n,s|\omega})\big) = 0, \ \forall k, s|\omega \tag{A.2a}$$

$$\kappa_{u,s|\omega} g^{up}_{u,s|\omega} = 0, \ \forall u, s|\omega \tag{A.2b}$$

$$\beta_{u,s|\omega}(G_u - g_{u,\omega} - g^{up}_{u,s|\omega}) = 0, \ \forall u, s|\omega \tag{A.2c}$$

$$\psi_{u,s|\omega} g^{dn}_{u,s|\omega} = 0, \ \forall u, s|\omega \tag{A.2d}$$

$$\varphi_{u,s|\omega}(g_{u,\omega} - g^{dn}_{u,s|\omega}) = 0, \ \forall u, s|\omega \tag{A.2e}$$

$$\theta_{n,s|\omega} v_{n,s|\omega} = 0, \ \forall n, s|\omega \tag{A.2f}$$

$$\chi_{n,s|\omega}(\bar{W}_{n,\omega} + \Delta W_{n,s|\omega} - v_{n,s|\omega}) = 0, \ \forall n, s|\omega \tag{A.2g}$$

We can prove that the strong duality condition in (B.1e) is the exact reformulation of the complementary slackness conditions in (A.2) using the following steps below:

Step 1 Multiply both sides of stationary conditions (B.1a), (B.1b) and (B.1c) by $g^{up}_{u,s|\omega}$, $g^{dn}_{u,s|\omega}$

and $v_{n,s|\omega}$, respectively. Sum the left-hand sides and obtain an equality which has a right-hand side value zero.

Step 2 Sum the both sides of all equalities in (A.2) and obtain an equality which has a right-hand side value zero.

Step 3 Subtract left-hand side of the equality obtained in Step 1 from the equality obtained in Step 2.

Step 4 From (A.1f), replace $\sum_{n:u}(g^{up}_{u,s|\omega} - g^{dn}_{u,s|\omega}) - v_{n,s|\omega}$ by $D_{n,\omega} - \Delta W_{n,s|\omega} - \sum_{n:u} g_{u,\omega}$. The resulting equality is exactly the same as (B.1e).

Given the day-ahead decisions, Table A.18 shows the bilinear terms and the number of constraints in two cases: (a) The KKT condition with complementary slackness conditions and (b) the KKT conditions with strong duality condition.

Table A.18: The bilinear terms and the number of constraints in Case (a) (KKT conditions with complementary slackness conditions) and in Case (b) (KKT conditions with strong duality condition), K: Number of transmission lines, U: Number of producers, N: Number of nodes, ΩxS: Number of imbalance scenarios.

	Location	Bilinear terms	#constraints	#bilinear terms
Case (a)	(A.1a)	$\hat{c}^{up}_{u,\omega} g^{up}_{u,s\|\omega}$	-*	S
		$\hat{c}^{dn}_{u,\omega} g^{dn}_{u,s\|\omega}$		S
	(A.2a)	$\mu_{k,s\|\omega} \sum_n H_{k,n}(\sum_u \Psi_{u,n} g^{up}_{u,s\|\omega})$ $\mu_{k,s\|\omega} \sum_n H_{k,n}(\sum_u \Psi_{u,n} g^{dn}_{u,s\|\omega})$ $\mu_{k,s\|\omega} \sum_n H_{k,n} v_{n,s\|\omega}$	KxΩxS	3xKxΩxS
	(A.2b)	$\kappa_{u,s\|\omega} g^{up}_{u,s\|\omega}$	UxΩxS	UxΩxS
	(A.2c)	$\beta_{u,s\|\omega} g^{up}_{u,s\|\omega}$	UxΩxS	UxΩxS
	(A.2d)	$\psi_{u,s\|\omega} g^{dn}_{u,s\|\omega}$	UxΩxS	UxΩxS
	(A.2e)	$\varphi_{u,s\|\omega} g^{dn}_{u,s\|\omega}$	UxΩxS	UxΩxS
	(A.2f)	$\theta_{n,s\|\omega} v_{n,s\|\omega}$	NxΩxS	NxΩxS
	(A.2g)	$\chi_{n,s\|\omega} v_{n,s\|\omega}$	NxΩxS	NxΩxS
Case (b)	(A.1a)	$\hat{c}^{up}_{u,\omega} g^{up}_{u,s\|\omega}$	-*	S
		$\hat{c}^{dn}_{u,\omega} g^{dn}_{u,s\|\omega}$		S
	(B.1e)	$\hat{c}^{up}_{u,\omega} g^{up}_{u,s\|\omega}$	ΩxS	UxΩxS
		$\hat{c}^{dn}_{u,\omega} g^{dn}_{u,s\|\omega}$		UxΩxS

It can be seen from Table A.18 that replacing the complementary slackness conditions by the strong duality conditions reduces the total number of constraints from $(K+4U+2N)$xΩxS to ΩxS. Moreover the number of bilinear terms reduces from $(3K + 4U + 2N)$xΩxS+2S to $2U$xΩxS+$2S$.

*Note that (A.1a) is the objective function of (A.1). Hence, it is not counted as a constraint.

Appendix B. The KKT conditions of (1) and (6)

Appendix B.1. The KKT conditions of (1)

The KKT conditions of (1) consists of the primal feasibility conditions, the stationary conditions, the dual feasibility conditions and the strong duality conditions. The primal feasibility conditions are illustrated in (1b)-(1f). The stationary conditions, the dual feasibility conditions and the strong duality conditions are illustrated in (B.1a)-(B.1c), (B.1d) and (B.1e), respectively.

$$-\sigma_{s|\omega}\hat{c}^{up}_{u,\omega} + \alpha_{s|\omega} - \sum_n \Psi_{u,n} \sum_k H_{k,n}\mu_{k,s|\omega} + \kappa_{u,s|\omega} - \beta_{u,s|\omega} = 0, \quad \forall u, s|\omega \tag{B.1a}$$

$$\sigma_{s|\omega}\hat{c}^{dn}_{u,\omega} - \alpha_{s|\omega} + \sum_n \Psi_{u,n} \sum_k H_{k,n}\mu_{k,s|\omega} + \psi_{u,s|\omega} - \varphi_{u,s|\omega} = 0, \quad \forall u, s|\omega \tag{B.1b}$$

$$-\alpha_{s|\omega} + \sum_k H_{k,n}\mu_{k,s|\omega} + \theta_{n,s|\omega} - \chi_{n,s|\omega} = 0, \quad \forall n, s|\omega \tag{B.1c}$$

$$\mu_{k,s|\omega}, \kappa_{u,s|\omega}, \beta_{u,s|\omega}, \psi_{u,s|\omega}, \varphi_{u,s|\omega}, \theta_{n,s|\omega}, \chi_{n,s|\omega} \geq 0 \tag{B.1d}$$

$$\begin{aligned} &\sum_u \sigma_{s|\omega}(-\hat{c}^{up}_{u,\omega}g^{up}_{u,s|\omega} + \hat{c}^{dn}_{u,\omega}g^{dn}_{u,s|\omega}) - (\alpha_{s|\omega}(\sum_u g_{u,\omega} - \sum_n (D_{n,\omega} - \Delta W_{n,s|\omega})) + \\ &\quad \sum_k \mu_{k,s|\omega}(F_k - \sum_n H_{k,n}(\sum_u \Psi_{u,n}g_{u,\omega} - D_{n,\omega} + \Delta W_{n,s|\omega})) + \sum_u (\varphi_{u,s|\omega}g_{u,\omega} + \\ &\quad \beta_{u,s|\omega}(G_u - g_{u,\omega})) + \sum_n \chi_{n,s|\omega}(W_{n,\omega} + \Delta W_{n,s|\omega})) = 0, \quad \forall s|\omega \end{aligned} \tag{B.1e}$$

Appendix B.2. The KKT conditions of (6)

The KKT conditions of (6) consists of the primal feasibility conditions, the stationary conditions, the dual feasibility conditions and the strong duality conditions. The primal feasibility conditions are illustrated in (6b)-(6i). The stationary conditions, the dual feasibility conditions and the strong duality conditions are illustrated in (B.2a)-(B.2l), (B.2m) and (B.2n), respectively.

$$\begin{aligned} &-\sigma_{s|\omega}\hat{c}^{up}_{u,\omega} + \lambda^A_s - \sum_n \Psi_{u,n} \sum_k H_{k,n}\lambda^B_{k,s} + \lambda^C_{u,s|\omega} - \lambda^D_{u,s|\omega} + \lambda^M_{u,s|\omega}\hat{c}^{up}_{u,\omega} - \\ &\quad C^{up}_u \lambda^M_{u,s|\omega} = 0, \quad \forall u, s|\omega \end{aligned} \tag{B.2a}$$

$$\begin{aligned} &\sigma_{s|\omega}\hat{c}^{dn}_{u,\omega} - \lambda^A_s + \sum_n \Psi_{u,n} \sum_k H_{k,n}\lambda^B_{k,s} + \lambda^E_{u,s|\omega} - \lambda^F_{u,s|\omega} - \lambda^M_{u,s|\omega}\hat{c}^{dn}_{u,\omega} + \\ &\quad C^{dn}_u \lambda^M_{u,s|\omega} = 0, \quad \forall u, s|\omega \end{aligned} \tag{B.2b}$$

$$-\lambda^A_s + \sum_k H_{k,n}\lambda^B_{k,s} + \lambda^G_{n,s|\omega} - \lambda^H_{n,s|\omega} = 0, \quad \forall n, s|\omega \tag{B.2c}$$

$$\sum_u (\lambda^I_{u,s|\omega} - \lambda^J_{u,s|\omega}) - \sum_n (\Delta W_{n,s|\omega} + \lambda^K_{n,s|\omega} + \lambda^L_{n,s|\omega}/\sigma_{s|\omega}) = 0, \quad \forall s \tag{B.2d}$$

$$\begin{aligned} &\sum_n H_{k,n}(\Delta W_{n,s|\omega} - D_{n,\omega} + \lambda^K_{n,s|\omega} + \lambda^L_{n,s|\omega}/\sigma_{s|\omega} + \sum_u \Psi_{u,n}(g_{u,\omega} - \lambda^I_{u,s|\omega} + \lambda^J_{u,s|\omega})) \\ &\quad - F_k + \lambda^N_{k,s|\omega} = 0, \quad \forall k, s|\omega \end{aligned} \tag{B.2e}$$

$$\lambda^I_{u,s|\omega} + \lambda^O_{u,s|\omega} = 0, \quad \forall u, s|\omega \tag{B.2f}$$

$$g_{u,\omega} - G_u - \lambda^I_{u,s|\omega} + \lambda^M_{u,s|\omega}(G_u - g_{u,\omega})/\sigma_{s|\omega} + \lambda^P_{u,s|\omega} = 0, \quad \forall u, s|\omega \tag{B.2g}$$

$$\lambda^J_{u,s|\omega} + \lambda^Q_{u,s|\omega} = 0, \quad \forall u, s|\omega \tag{B.2h}$$

$$- g_{u,\omega} - \lambda^J_{u,s|\omega} + \lambda^M_{u,s|\omega} g_{u,\omega}/\sigma_{s|\omega} + \lambda^R_{u,s|\omega} = 0, \quad \forall u, s|\omega \tag{B.2i}$$

$$\lambda^K_{u,s|\omega} + \lambda^S_{u,s|\omega} = 0, \quad \forall n, s|\omega \tag{B.2j}$$

$$- (W_{n,\omega} + \Delta W_{n,\omega}, s) - \lambda^K_{n,s|\omega} + \lambda^T_{n,s|\omega} = 0, \quad \forall n, s|\omega \tag{B.2k}$$

$$\sum_n -\tilde{\Psi}_{n,z}\lambda^L_{n,s|\omega} = 0, \quad \forall z, s|\omega \tag{B.2l}$$

$$\lambda^B_{k,s|\omega}, \lambda^C_{u,s|\omega}, \lambda^D_{u,s|\omega}, \lambda^E_{u,s|\omega}, \lambda^F_{u,s|\omega}, \lambda^G_{u,s|\omega}, \lambda^H_{u,s|\omega}, \lambda^M_{u,s|\omega}, \lambda^N_{k,s|\omega}, \lambda^O_{u,s|\omega}, \lambda^P_{u,s|\omega}, \lambda^Q_{u,s|\omega},$$
$$\lambda^R_{u,s|\omega}, \lambda^S_{n,s|\omega}, \lambda^T_{n,s|\omega} \geq 0 \tag{B.2m}$$

$$\sum_u \sigma_{s|\omega}(-\hat{c}^{up}_{u,\omega} g^{up}_{u,s|\omega} + \hat{c}^{dn}_{u,\omega} g^{dn}_{u,s|\omega}) - (\alpha_{s|\omega}(\sum_u g_{u,\omega} - \sum_n (D_{n,\omega} - \Delta W_{n,s|\omega})) +$$
$$\sum_k \mu_{k,s|\omega}(F_k - \sum_n H_{k,n}(\sum_u \Psi_{u,n} g_{u,\omega} - D_{n,\omega} + \Delta W_{n,s|\omega})) + \sum_u (\varphi_{u,s|\omega} g_{u,\omega} +$$
$$\beta_{u,s|\omega}(G_u - g_{u,\omega})) + \sum_n \chi_{n,s|\omega}(W_{n,\omega} + \Delta W_{n,s|\omega})) - (\lambda^A_s(\sum_u g_{u,\omega} -$$
$$\sum_n (D_{n,\omega} - \Delta W_{n,s|\omega})) + \sum_k \lambda^B_{k,s|\omega}(F_k - \sum_n H_{k,n}(\sum_u \Psi_{u,n} g_{u,\omega} - D_{n,\omega} +$$
$$\Delta W_{n,s|\omega})) + \sum_u (\lambda^D_{u,s|\omega}(G_u - g_{u,\omega}) + \lambda^F_{u,s|\omega} g_{u,\omega} - \sigma_{s|\omega}\hat{c}^{up}_{u,\omega}\lambda^I_{u,s|\omega} +$$
$$\sigma_{s|\omega}\hat{c}^{dn}_{u,\omega}\lambda^J_{u,s|\omega}) + \sum_n \lambda^H_{n,s|\omega}(W_{n,\omega} + \Delta W_{n,s|\omega})) = 0, \quad \forall s|\omega \tag{B.2n}$$